



Scientific Analysis/Calculation Administrative Change Notice

QA: QA
Page 1 of 3

Complete only applicable items.

1. Document Number:	ANL-NBS-HS-000047	2. Revision:	01	3. ACN:	01
4. Title:	THC Sensitivity Study of Heterogeneous Permeability and Capillarity Effects				
5. No. of Pages Attached:	35				

6. Approvals:	
Preparer:	<div style="display: flex; justify-content: space-between;"> <div style="text-align: center;"> <u>S. Mukhopadhyay</u> <i>S. Mukhopadhyay</i> Print Name and Sign </div> <div style="text-align: center;"> <u>01/10/2008</u> Date </div> </div>
Checker:	<div style="display: flex; justify-content: space-between;"> <div style="text-align: center;"> <u>C. Ho</u> <i>Clifford K. Ho</i> Print name and sign </div> <div style="text-align: center;"> <u>1/10/2008</u> Date </div> </div>
QCS/Lead Lab QA Reviewer:	<div style="display: flex; justify-content: space-between;"> <div style="text-align: center;"> <u>R. Spencer</u> <i>Robert Spencer</i> Print name and sign </div> <div style="text-align: center;"> <u>1/11/08</u> Date </div> </div>
Responsible Manager:	<div style="display: flex; justify-content: space-between;"> <div style="text-align: center;"> <u>K. Knowles</u> <i>K. Knowles</i> Print name and sign </div> <div style="text-align: center;"> <u>1/11/08</u> Date </div> </div>
7. Affected Pages	8. Description of Change:
iv	Added Acknowledgements page (page iva) after existing page iv.
ix	<p>Table of Figures: Updated listing for Figure 6.3-1 to reflect change in corresponding figure caption (see change description for page 6-10).</p> <p>Table of Figures: Updated listing for Figure 6.6-2 to reflect change in corresponding figure caption (see change description for page 6-47).</p> <p>Table of Figures: Updated listing for Figure 6.6-3 to reflect change in corresponding figure caption (see change description for page 6-48).</p>
x	<p>Table of Figures: Updated listing for Figure 6.7-1 to reflect change in corresponding figure caption (see change description for page 6-74).</p> <p>Table of Figures: Updated listing for Figure 6.7-2 to reflect change in corresponding figure caption (see change description for page 6-75).</p> <p>Table of Figures: Updated listing for Figure 6.7-3 to reflect change in corresponding figure caption (see change description for page 6-76).</p> <p>Table of Figures: Updated listing for Figure 6.7-4 to reflect change in corresponding figure caption (see change description for page 6-82).</p> <p>Table of Figures: Updated listing for Figure 6.7-5 to reflect change in corresponding figure caption (see change description for page 6-83).</p> <p>Table of Figures: Updated listing for Figure 6.7-6 to reflect change in corresponding figure caption (see change description for page 6-84).</p>
1-1	Section 1.1, third paragraph: Revised and combined last two sentences as follows: "The ultimate goal of these sensitivity analyses is to evaluate the effects from THC processes on the predicted occurrence of seepage, and to provide sufficient technical bases for increasing confidence in the abstraction of drift seepage."
2-1	Second paragraph, bulleted list: Replaced existing bulleted items with "Upper natural barrier (unsaturated zone above the repository)" and "Lower natural barrier (unsaturated zone below the repository)".



Scientific Analysis/Calculation Administrative Change Notice

Complete only applicable items.

1. Document Number:	ANL-NBS-HS-000047	2. Revision:	01	3. ACN:	01
4. Title:	THC Sensitivity Study of Heterogeneous Permeability and Capillarity Effects				
6-2	Section 6.1.1, first paragraph: Replaced “tunnels” with “drifts” in first sentence; replaced “tunnel” with “drift” in third sentence.				
6-4	First paragraph: Replaced “tunnel” with “drift” in last sentence.				
6-5	Second paragraph: Replaced “tunnel” with “drift” in third sentence; replaced “tunnels” with “drifts” in fourth sentence. Section 6.1.2, first paragraph: Replaced “tunnels” with “drifts” in first and third sentences. Section 6.1.2, Second paragraph: Replaced “tunnel” with “drift” in first sentence; replaced “tunnels” with “drifts” in second sentence.				
6-6	First full paragraph: Replaced “tunnel” with “drift” in third sentence. Second paragraph: Replaced “tunnels” with “drifts” in first sentence.				
6-8	Section 6.3, first paragraph: Replaced “tunnel” with “drift” in first four sentences; replaced “tunnel” with “drift” and “tunnels” with “drifts” in last sentence. Section 6.3, second paragraph: Replaced “tunnel” with “drift” in third sentence.				
6-10	Figure 6.3-1: Replaced “Tunnel” with “Drift” in figure caption.				
6-14	Section 6.4.2, first paragraph: Replaced “tunnel” with “drift” in next-to-last sentence.				
6-18	Section 6.4.6, first paragraph: Replaced “tunnels” with “drifts” in last sentence.				
6-28	Section 6.4.11.2, first paragraph, second bulleted item: Replaced “tunnels” with “drifts”. Section 6.4.11.2, second paragraph: Replaced “tunnel” with “drift” in second sentence.				
6-29	First bulleted item: Replaced “tunnel” with “drift”.				
6-38	Section 6.5.1, first paragraph: Added the following after second sentence: “The numerical difficulty encountered by this simulation is specific to this simulation only, and has no impact on other simulations in this report. Recollect that different realizations of the same fracture permeability distribution are used in this report. For this particular simulation with Realization # 1 of the permeability distribution, the initial permeability of a few gridblocks and their spatial/temporal evolution were such that it resulted in a singular matrix in the chemical solver routine of the software TOUGHREACT. Thus non-convergence for this simulation was not because of any coding or data-entry error but because of a rare occurrence.”				
6-43	First paragraph: Replaced “tunnel” with “drift” in first sentence.				
6-46	Section 6.6.2, last bulleted item, second sentence: Replaced existing sentence with “Note that results from the corresponding THC simulation (Simulation ID: “base_r1_10x_lev_thc”) are not available (see Tables 6.5-2 and 6.6-1), as explained in Section 6.5.1”. Section 6.6.2, last bulleted item, last sentence: Replaced parenthetical statement with “(i.e., ten times the infiltration fluxes of the glacial transition period)”.				
6-47	Figure 6.6-2: Replaced existing figure to remove climate-period demarcations; added a closing parenthesis after “(Simulation ID “base_r1_10x_lev_amb” in figure caption; added “with IMF10 Infiltration Fluxes” at the end of caption; deleted sentence “The vertical violet lines are used to distinguish the different climatic periods and they do not represent any seepage data” in figure note.				



Scientific Analysis/Calculation Administrative Change Notice

QA: QA
Page 3 of 3

Complete only applicable items.

1. Document Number:	ANL-NBS-HS-000047	2. Revision:	01	3. ACN:	01
4. Title:	THC Sensitivity Study of Heterogeneous Permeability and Capillarity Effects				
6-48	Figure 6.6-3: Replaced existing figure to remove climate-period demarcations; added “with IMF10 Infiltration Fluxes” at the end of figure caption; deleted sentence “The vertical violet lines are used to distinguish the different climatic periods and they do not represent any seepage data” in figure note. Section 6.6.2, first paragraph, lines 3 and 4: Added “effect” after “capillary-barrier”. Section 6.6.2, second paragraph, line 4: Changed “simulations shows” to “simulations show”.				
6-49	Section 6.6.2, second bulleted item, last line: Added “computed” after “capillary-barrier effects”.				
6-53	Section 6.6.3, fourth paragraph, fifth line: Changed “though” to “through”.				
6-74	Figure 6.7-1: Replaced existing figure to remove climate-period demarcations; added “with IMF10 Infiltration Fluxes” at the end of figure caption; deleted sentence “The vertical violet lines are used to distinguish the different climatic periods and they do not represent any seepage data” in figure note.				
6-75	Figure 6.7-2: Replaced existing figure to remove climate-period demarcations; added “with IMF10 Infiltration Fluxes” at the end of figure caption; deleted sentence “The vertical violet lines are used to distinguish the different climatic periods and they do not represent any seepage data” in figure note.				
6-76	Figure 6.7-3: Replaced existing figure to remove climate-period demarcations; added “with IMF10 Infiltration Fluxes” at the end of figure caption; deleted sentence “The vertical violet lines are used to distinguish the different climatic periods and they do not represent any seepage data” in figure note.				
6-82	Figure 6.7-4: Replaced existing figure to remove climate-period demarcations; added “with IMF10 Infiltration Fluxes” at the end of figure caption; deleted sentence “The vertical violet lines are used to distinguish the different climatic periods and they do not represent any seepage data” in figure note.				
6-83	Figure 6.7-5: Replaced existing figure to remove climate-period demarcations; added “with IMF10 Infiltration Fluxes” at the end of figure caption; deleted sentence “The vertical violet lines are used to distinguish the different climatic periods and they do not represent any seepage data” in figure note.				
6-84	Figure 6.7-6: Replaced existing figure to remove climate-period demarcations; added “with IMF10 Infiltration Fluxes” at the end of figure caption; deleted sentence “The vertical violet lines are used to distinguish the different climatic periods and they do not represent any seepage data” in figure note.				
6-90	Section 6.10, first paragraph, second to last sentence: Replaced existing sentence with “These simulations improve confidence with regard to seepage estimation under THC conditions”. Section 6.11, second paragraph, third sentence: Replaced existing sentence with “As mentioned in Section 1.1, the objective of these sensitivity studies is to improve confidence in the abstraction of drift seepage”.				
7-1	Section 7.1, second paragraph: Replaced “tunnels” with “drifts” in fourth sentence.				
7-4	Section 7.2, third sentence: Replaced existing sentence with “The objective of this work is to increase confidence in the abstraction of drift seepage (BSC 2004 [DIRS 169131]), which supports TSPA (Section 1.1)”.				
7-5	First full paragraph, second sentence: Replaced existing sentence with “Additional sensitivity studies could further improve confidence in seepage calculations.” First full paragraph, last sentence: Replaced existing sentence with “Notwithstanding these opportunities to further increase model confidence, the primary conclusions of this report would not be expected to change significantly.”				

ACKNOWLEDGEMENTS

This study was conducted at Lawrence Berkeley National Laboratory, Earth Sciences Division.

Nicolas Spycher, Guoxiang Zhang, Stefan Finsterle, and Eric Sonnenthal contributed to the technical contents of this report.

We would like to acknowledge technical data coordination by Carol Valladao, technical review by Ernest Hardin and Prasad Nair, and help in tracking and checking technical inputs by Emma Thomas.

Production and technical editing assistance by Tom Breene, Dan Hawkes, Krys Avina, and Lisa Feedar are also duly acknowledged.

FIGURES

	Page
6.1-1. Schematic of TH Processes at the Drift Scale and the Mountain Scale	6-3
6.1-2. Schematic Diagram of Fracture–Matrix Interface Showing the Relationship between TH Processes and Geochemical Processes	6-4
6.1-3. Schematic Representation of Interplay of THC Processes, Local Flow Channeling, and Seepage	6-7
6.3-1. Schematic Representation of Seepage into an Emplacement Drift Situated in Unsaturated Fractured Rock	6-10
6.4-1. 2-D Numerical Grid Used in Ambient, TH, and THC Simulations with the Drift-Scale THC Seepage Model (SNL 2007 [DIRS 177404])	6-15
6.4-2. Transient Thermal Loading History of the Emplaced Wastes at Yucca Mountain...	6-17
6.4-3. Heterogeneous Fracture Permeability Distribution for Realization #1 at the Start of Ambient/TH/THC Simulations	6-26
6.4-4. Three-Dimensional Data-Generation Model: (a) Log-Permeability Field, (b) Liquid Saturation after 30 Days of Liquid Release	6-33
6.4-5. Two-Dimensional Calibration Model: (a) One Realization of Log-Permeability Field, (b) Liquid Saturation after 30 Days of Liquid Release	6-34
6.4-6. Synthetic Seepage-Rate Data (symbols) and Matches Obtained by Two- Dimensional Calibration Models Using 20 Realizations of the Small-Scale Permeability Field: (a) without Leverett Scaling, (b) with Leverett Scaling	6-35
6.4-7. Histogram of Estimated Capillary-Strength Parameter Obtained with 20 Different Calibration Models: (a) without Leverett Scaling, (b) with Leverett Scaling	6-35
6.6-1. Sample Contours of Temperature above and below the Emplacement Drift.....	6-42
6.6-2. Comparison of Seepage Fluxes from Ambient (Simulation ID: “base_r1_10x_lev_amb”) and TH (Simulation ID: “base_r1_10x_lev_th”) Simulations with IMF10 Infiltration Fluxes.....	6-47
6.6-3. Comparison of Seepage Fluxes from Ambient (Simulation ID: “base_r2_10x_lev_amb”), TH (Simulation ID “base_r2_10x_lev_th.”), and THC (Simulation ID: “base-r2_10x_lev_thc”) Simulations with IMF10 Infiltration Fluxes	6-48
6.6-4. Location of Model Gridblocks for Data Shown on Figures 6.6-5 through 6.6-17....	6-55
6.6-5. Time Profiles of Modeled Temperatures in Water above the Drift in Fractures and inside the Drift	6-56
6.6-6. Time Profiles of Modeled Liquid Saturations in Water above the Drift in Fractures and inside the Drift	6-57
6.6-7. Time Profiles of Modeled Total Aqueous Chloride Concentrations in Water above the Drift in Fractures and inside the Drift.....	6-58
6.6-8. Time Profiles of Modeled CO ₂ Gas Concentrations above and inside the Drift.....	6-59
6.6-9. Time Profiles of Modeled pH in Water above the Drift in Fractures and inside the Drift	6-60
6.6-10. Time Profiles of Modeled Total Aqueous Carbonate Concentrations in Water above the Drift in Fractures and inside the Drift.....	6-61

FIGURES (Continued)

	Page
6.6-11. Time Profiles of Modeled Total Aqueous Calcium Concentrations in Water above the Drift in Fractures and inside the Drift.....	6-62
6.6-12. Time Profiles of Modeled Total Aqueous Magnesium Concentrations in Water above the Drift in Fractures and inside the Drift.....	6-63
6.6-13. Time Profiles of Modeled Total Aqueous Sodium Concentrations in Water above the Drift in Fractures and inside the Drift.....	6-64
6.6-14. Time Profiles of Modeled Total Aqueous Sodium to Chloride Concentration Ratios in Water above the Drift in Fractures and inside the Drift.....	6-65
6.6-15. Time Profiles of Modeled Total Aqueous Potassium Concentrations in Water above the Drift in Fractures and inside the Drift.....	6-66
6.6-16. Time Profiles of Modeled Total Aqueous Nitrate Concentrations in Water above the Drift in Fractures and inside the Drift	6-67
6.6-17. Time Profiles of Modeled Total Aqueous Sulfate Concentrations in Water above the Drift in Fractures and inside the Drift.....	6-68
6.6-18. Time Profiles of Modeled Total Aqueous Nitrate to Chloride Concentrations in Water above the Drift in Fractures and inside the Drift	6-69
6.7-1. Comparison of Seepage Fluxes from Ambient (Simulation ID: “scm_r1_10x_nlev_amb”), TH (Simulation ID: “scm_r1_10x_nlev_th.”), and THC (Simulation ID: “scm_r1_10x_nlev_thc”) Simulations with Realization #1 of the Heterogeneous Fracture Permeability Distribution with IMF10 Infiltration Fluxes.....	6-74
6.7-2. Comparison of Seepage Fluxes from Ambient (Simulation ID: “scm_r2_10x_nlev_amb”), TH (Simulation ID: “scm_r2_10x_nlev_th.”), and THC (Simulation ID: “scm_r2_10x_nlev_thc”) Simulations with Realization #2 of the Heterogeneous Fracture Permeability Distribution with IMF10 Infiltration Fluxes.....	6-75
6.7-3. Seepage Fluxes from THC (Simulation ID: “scm_r3_10x_nlev_thc”) Simulations with Realization #3 of the Heterogeneous Fracture Permeability Distribution with IMF10 Infiltration Fluxes	6-76
6.7-4. Comparison of Seepage Fluxes from Ambient (Simulation ID: “itr_r1_10x_lev_amb”), TH (Simulation ID: “itr_r1_10x_lev_th.”), and THC (Simulation ID: “itr_r1_10x_lev_thc”) Simulations with Realization #1 of the Heterogeneous Fracture Permeability Distribution and Initial Fracture Capillary-strength Parameter of 1,313 Pa (see Section 6.7.2.1 and Table 6.7–4) with IMF10 Infiltration Fluxes.....	6-82
6.7-5. Comparison of Seepage Fluxes from Ambient (Simulation ID: “tr_r2_10x_lev_amb”), TH (Simulation ID: “itr_r2_10x_lev_th.”), and THC (Simulation ID: “itr_r2_10x_lev_thc”) Simulations with Realization #2 of the Heterogeneous Fracture Permeability Distribution and Initial Fracture Capillary-strength Parameter of 2,000 Pa (see Section 6.7.2.1 and Table 6.7–4) with IMF10 Infiltration Fluxes.....	6-83

FIGURES (Continued)

	Page
6.7-6. Comparison of Seepage Fluxes from Ambient (Simulation ID: “itr_r3_10x_lev_amb”), TH (Simulation ID: “itr_r3_10x_lev_th.”), and THC (Simulation ID: “itr_r3_10x_lev_thc”) Simulations with Realization #3 of the Heterogeneous Fracture Permeability Distribution and Initial Fracture Capillary-strength Parameter of 750 Pa (see Section 6.7.2.1 and Table 6.7-4) with IMF10 Infiltration Fluxes.....	6-84
A.1-1. Organization of Folders in DTN: LB0705THCSENHF.001.....	A.1-2
A.2-1. Organization Chart of Folders Containing STEADY and THC Simulation Input and Output Files	A.2-4

1. PURPOSE

1.1 OBJECTIVE

The purpose of this report is to document the sensitivity of the drift-scale thermal-hydrologic-chemical (THC) seepage model (SNL 2007 [DIRS 177404]) to heterogeneities in permeability and capillarity, which could affect predicted fluxes and chemistries of water and gases seeping into the emplacement drifts. This report has been developed following *Technical Work Plan for: Revision of Model Reports for Near-Field and In-Drift Water Chemistry* (SNL 2007 [DIRS 179287]). Furthermore, this report has been prepared in accordance with the latest version of SCI-PRO-005, *Scientific Analyses and Calculations*.

This is a revision of the analysis report *THC Sensitivity Study of Repository Edge and Heterogeneous Permeability Effects* (BSC 2006 [DIRS 174104]), hereafter referred to as the THC Sensitivity Study. In accordance with *Technical Work Plan for: Revision of Model Reports for Near-Field and In-Drift Water Chemistry* (SNL 2007 [DIRS 179287], Section 1.1), the present revision of the THC sensitivity study will be called *THC Sensitivity Study of Heterogeneous Permeability and Capillarity Effects*, as it no longer addresses the repository edge effects. Per the technical work plan (TWP) (SNL 2007 [DIRS 179287], Section 1.1), the analyses pertaining to repository edge effects have been moved to the model report *Drift-Scale THC Seepage Model* (SNL 2007 [DIRS 177404]).

The objective of this report is to address in part Condition Report (CR) 7037, which notes that information provided in Revision 00 of the THC sensitivity study (BSC 2006 [DIRS 174104]) shows that predicted seepage is enhanced by THC effects not considered in *Abstraction of Drift Seepage* (BSC 2004 [DIRS 169131]). The observations in the THC sensitivity study were based on limited analyses (such as relying only on one realization of the heterogeneous fracture permeability distribution) of the THC seepage model sensitivity to permeability heterogeneities. The THC sensitivity study also did not account for the corresponding changes in fracture capillarity associated with spatially/temporally variable fracture permeability distributions. The revised analysis in the present report is based on a more comprehensive evaluation of the sensitivity of the THC seepage model to heterogeneities, both in fracture permeability and capillarity. It also documents the sensitivity of the THC seepage model through implementation of multiple realizations of the heterogeneous fracture permeability distribution, multiple initial fracture capillary-strength parameters of the host rock, and enhanced infiltration fluxes. The ultimate goal of these sensitivity analyses is to evaluate the effects from THC processes on the predicted occurrence of seepage, and to provide sufficient technical bases for increasing confidence in the abstraction of drift seepage.

1.2 OVERVIEW OF THE THC SEEPAGE MODEL

The drift-scale THC seepage model has been fully documented and validated in *Drift-Scale THC Seepage Model* (SNL 2007 [DIRS 177404]). The model provides an analysis of the effects of coupled thermal, hydrological, and chemical processes on infiltration water chemistry and gas-phase composition in the near-field host rock around waste emplacement drifts. The model

includes a complete description of the pertinent mineral–water processes in the host rock and their effect on the near-field environment. It is used to evaluate the effects of mineral dissolution

2. QUALITY ASSURANCE

Development of this report and the supporting analyses activities have been determined to be subject to the Yucca Mountain Project's Quality Assurance Program as indicated in *Technical Work Plan for: Revision of Model Reports for Near-Field and In-Drift Water Chemistry* (SNL 2007 [DIRS 179287]). Approved quality assurance implementing procedures identified in the TWP (SNL 2007 [DIRS 179287], Section 4) have been used to conduct and document the activities described in this report. The main governing procedure for this document was SCI-PRO-005, *Scientific Analyses and Calculations*. An evaluation in accordance with IM-PRO-002, *Control of the Electronic Management of Information*, has been conducted, and this work is subject to requirements to manage and control electronic data. The evaluation was submitted to the Records Processing Center as part of the TWP records package.

This report is intended to complement results of the THC seepage model, presented in *Drift-Scale THC Seepage Model* (SNL 2007 [DIRS 177404]). This report investigates the effect of drift-scale THC processes on the following safety category barriers that are important to the demonstration of compliance with the postclosure performance objective prescribed in 10 CFR 63.113 [DIRS 173273]:

- Upper natural barrier (unsaturated zone above the repository)
- Lower natural barrier (unsaturated zone below the repository).

The barriers are classified as "Safety Category" with regard to importance to waste isolation as defined in *Q-List* (BSC 2005 [DIRS 175539]). The report contributes to the analyses and modeling data used to support the total system performance assessment (TSPA), but is not directly used by TSPA. The conclusions from this report do not directly impact the engineered features important to preclosure safety as defined in LS-PRO-0203.

Table 6-1. Features, Events, and Processes Associated with This Report (Continued)

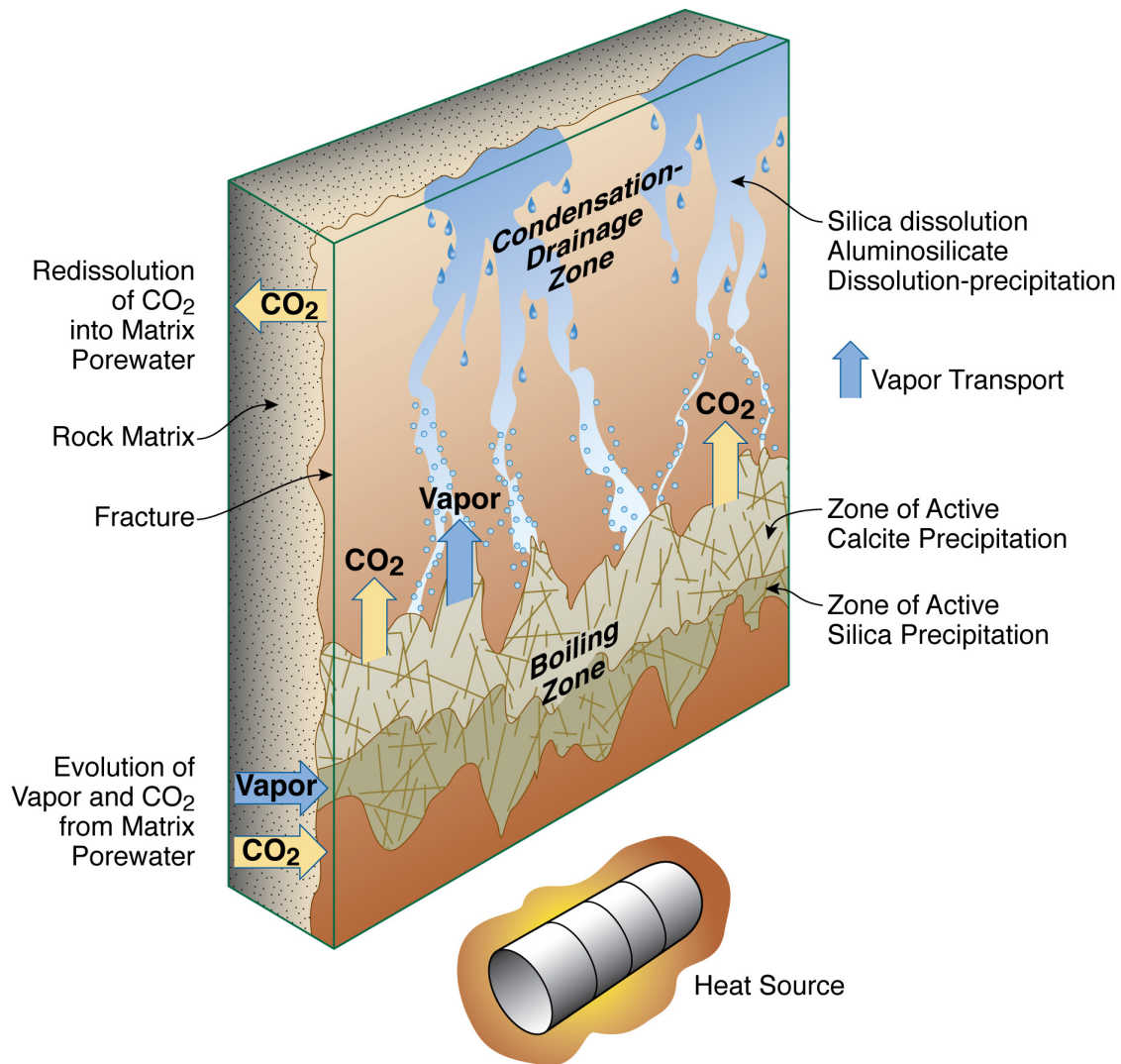
FEP No.	FEP Name	FEP Description	Sections Discussing FEPs-Related Items
2.210.01.0A	Repository-Induced Thermal Effects on Flow in the UZ	Thermal effects in the geosphere could affect the long-term performance of the disposal system, including effects on groundwater flow (e.g., density-driven flow), mechanical properties, and chemical effects in the UZ.	6.1.1, 6.1.2, 6.3, 6.4.4, 6.6.1, 6.6.2, 6.6.3, 6.7.1, 6.7.2, 6.8, 6.9, 6.10, 7.1, and 7.2

6.1 OVERVIEW

6.1.1 TH and THC Processes

Emplacement of hot waste packages in underground drifts is expected to cause various coupled thermal-hydrological-chemical (THC) processes in the unsaturated, fractured host rock. Focusing first on coupled thermal-hydrological (TH) processes (Figure 6.1-1), it is expected that the heat will cause vaporization and boiling of the matrix pore water, with subsequent migration of vapor out of the matrix into the embedded fractures. Once in the fracture, water vapor will move away from the drift through the permeable fracture network by buoyancy, by the increased vapor pressure resulting from heating and boiling, and by local convection. In cooler regions, vapor will condense on fracture walls, where it will flow through the fracture network under gravity drainage or be absorbed back into the matrix (because of the stronger capillarity of the matrix pores). Slow imbibition of water from fractures into the matrix gradually leads to increases in the liquid saturation of the rock matrix. Under conditions of continuous thermal loading, a dryout zone will eventually develop closest to the heat source, separated from the condensation zone by a nearly isothermal zone maintained at about the boiling temperature of water. This nearly isothermal zone is characterized by a continuous process of boiling, vapor transport, condensation, and migration of water back to the heat source (either by capillary forces or gravity drainage), often called a heat pipe (Pruess et al. 1990 [DIRS 100819]). TH processes in the unsaturated fractured rocks of Yucca Mountain have been extensively examined since the early 1980s (Pruess et al. 1984 [DIRS 144801]; Pruess et al. 1990 [DIRS 100819]; Buscheck and Nitao 1993 [DIRS 100617]; Pruess 1997 [DIRS 144794]; Kneafsey and Pruess 1998 [DIRS 139133]; Haukwa et al 1999 [DIRS 137562]; Buscheck et al. 2002 [DIRS 160749]; Haukwa et al. 2003 [DIRS 165165]; Birkholzer et al. 2004 [DIRS 172262]; BSC 2005 [DIRS 172232]; BSC 2005 [DIRS 174101]; Wu et al. 2006 [DIRS 180274]). The methods used in these predictive studies have also been validated against the TH response of heater tests conducted at the repository site (Tsang and Birkholzer 1999 [DIRS 137577]; Birkholzer and Tsang 2000 [DIRS 154608]; Mukhopadhyay and Tsang 2002 [DIRS 160788]; Mukhopadhyay and Tsang 2003 [DIRS 160790]; BSC 2005 [DIRS 172232]).

condensate in the fracture system determines where mineral dissolution and precipitation can occur in the fractures and where there can be direct interaction (via diffusion) between matrix pore waters and fracture waters. Figure 6.1-2 schematically shows the relationships between TH and chemical processes in the zones of boiling, condensation, and drainage, in the rock mass at the fracture–matrix interface surrounding an emplacement drift.



NW07-015

Figure 6.1-2. Schematic Diagram of Fracture–Matrix Interface Showing the Relationship between TH Processes and Geochemical Processes

In short, redistribution of mineral phases will occur as a result of differences in mineral solubility as a function of temperature. The inverse relation between temperature and calcite solubility (as opposed to the silica phases, which are more soluble at higher temperatures) will also cause zonation in the distribution of calcite and silica phases in both the condensation and boiling zones (Figure 6.1-2). Precipitation of amorphous silica or another silica phase is likely to be confined to a narrower zone, where the evaporative concentration from boiling exceeds its solubility. In contrast, calcite could precipitate in fractures over a broad zone of elevated

temperature and where CO₂ has exsolved because of temperature increases or boiling. Alteration of feldspars to clays and zeolites is likely to be most rapid in the boiling zone because of their increased solubility (as well as higher dissolution and precipitation fluxes) at higher temperatures (Lasaga 1998 [DIRS 117091]). Coupled THC processes in the unsaturated fractured rock of Yucca Mountain have been under investigation for some time now (Spycher et al. 2003 [DIRS 162121]; Sonnenthal et al. 2005 [DIRS 176005]; BSC 2006 [DIRS 174104]; Mukhopadhyay et al. 2006 [DIRS 180822]; SNL 2007 [DIRS 177404]). These THC modeling studies investigate the coupling among heat, water, and vapor flow, aqueous and gaseous species transport, kinetic and equilibrium mineral–water reactions, and feedback of mineral precipitation/dissolution on porosity, permeability, and capillary pressure. Such studies developed the underlying conceptual and mathematical models, which provide the basis for modeling the TH effects of the relevant mineral-water-gas reactions and transport processes in the host rock.

While the overall impact of THC processes in unsaturated fractured rock has been dealt with in those previous investigations, this report focuses on one particular aspect—the changes in the hydrologic properties of the unsaturated fractured rock, caused by the THC processes. THC processes of mineral precipitation and dissolution dynamically change the hydraulic properties of the rock (such as porosity, permeability, and capillary characteristics). These changes, in turn, cause perturbations in the flow fields around an emplacement drift, which may lead to local flow channeling. In this report, it is shown that simulations may predict seepage (i.e., dripping of liquid water from the unsaturated rock into the emplacement drifts) because of such local flow channeling, depending on how changes in capillary response are represented.

6.1.2 Seepage

Seepage refers to dripping of liquid water into the emplacement drifts from the rock above. Understanding the processes affecting seepage is important, because seepage (or its absence) is directly connected to the overall performance of a repository in successfully isolating nuclear waste from the geosphere. For example, if seepage occurs, it may promote corrosion of the waste packages, which may lead to release of radioactive materials from the emplacement drifts into the surrounding rock. Both experimental and modeling analyses (Wang et al. 1999 [DIRS 106146]; Trautz and Wang 2002 [DIRS 160335]; Finsterle et al. 2003 [DIRS 163214]; BSC 2004 [DIRS 171764]) have been performed to determine the processes affecting seepage under ambient conditions, i.e., in the absence of any thermal effects. Predictive modeling studies, based on a stochastic continuum model, have also been carried out to predict the probability and magnitude of seepage under ambient conditions at Yucca Mountain (Li and Tsang [DIRS 163714]; BSC 2004 [DIRS 167652]).

These previous ambient seepage studies have generally concluded that seepage under ambient conditions is reduced or prevented by the “capillary-barrier” effect (i.e., the difference in capillary pressure between the rock formation and a large underground opening such as the emplacement drift). This capillary-barrier effect causes water to be mostly diverted around the drifts rather than seeping into them. However, according to those earlier investigations, seepage under ambient conditions can still occur when local flow channeling, caused by heterogeneities in the host rock, results in local saturation buildup. If saturation buildup exceeds a certain

threshold saturation (see below for further discussion), the capillary barrier is overcome, and seepage commences. Thus, heterogeneity plays a crucial role in controlling seepage.

Since spent fuel waste can impose considerable thermal load on the surrounding rock, seepage under thermal conditions has also been investigated at Yucca Mountain through development of TH seepage models (Birkholzer et al. 2004 [DIRS 172262]; BSC 2005 [DIRS 172232]). While the capillary-barrier effect and heterogeneity of the host rock were found to control seepage even under thermal conditions (similar to ambient seepage), some significant differences in the mechanism of seepage between the two were also observed. The superheated dryout zone outside the emplacement drift under thermal conditions subjected incoming water to vigorous boiling, preventing liquid water from reaching the drift (i.e., liquid water could reach the drift wall only after the dryout zone had disappeared). In other words, the dryout zone provides an additional barrier to seepage, effectively creating what has been termed a “vaporization barrier” (Birkholzer et al. 2004 [DIRS 172262]; BSC 2005 [DIRS 172232]). While the analyses in the study by Birkholzer et al. (2004 [DIRS 172262]) and in *Drift-Scale Coupled Processes (DST and TH Seepage) Models* (BSC 2005 [DIRS 172232]) provide an important framework for investigating seepage including TH effects, the THC changes in the host rock are not included in their conceptual model. It has only recently been shown (BSC 2006 [DIRS 174104]; Mukhopadhyay et al. 2006 [DIRS 180822]) that the THC conditions in the rock are pertinent for seepage, not only for the chemistry of the seepage water but also for the amount and duration of seepage. As stated earlier, heterogeneity in the host rock plays a key role in controlling seepage. By changing the hydrologic properties of the rock, the THC processes introduce dynamic (i.e., time-dependent) heterogeneities in the rock. Thus, the transient pattern of seepage under THC processes is different from that when only ambient or TH processes are considered.

The feedback of the THC processes on the hydrologic properties of the rock has been shown (BSC 2006 [DIRS 174104]; Mukhopadhyay et al. 2006 [DIRS 180822]) to cause alteration of the flow pattern near the emplacement drifts, resulting in seepage under some circumstances. However, the analyses in *THC Sensitivity Study of Repository Edge and Heterogeneous Permeability Effects* (BSC 2006 [DIRS 174104]) and in the study by Mukhopadhyay et al. (2006 [DIRS 180822]) were performed assuming dynamic changes in permeability and porosity only, i.e., the feedback of THC processes was restricted to only those two hydrologic properties. However, mineral precipitation and dissolution also alter the capillary characteristics of the rock, which have a direct impact on flow channeling and seepage (see Figure 6.1-3 for a schematic representation of THC processes, local flow channeling, and seepage). In this report, simulations are performed to analyze the feedback of THC processes on the hydrologic properties (porosity, permeability, and capillarity) of the rock and ultimately on seepage. Ambient and TH simulations are also performed to illustrate the difference between these processes in the context of seepage (or its absence).

Seepage under ambient conditions has been extensively investigated in *Seepage Model for PA Including Drift Collapse* (BSC 2004 [DIRS 167652]). Seepage has also been found to occur under thermal conditions in *Drift-Scale Coupled Process (DST and TH Seepage) Models* (BSC 2005 [DIRS 172232]). This latter report analyzed the TH conditions in the near-field rock and provided estimates of seepage into drifts. However, in estimating duration and amount of seepage into the drifts, the report did not include the impact of THC changes in the near-field rock, which might impact seepage into drifts. Alongside ambient and TH seepage models, drift-scale THC seepage models (SNL 2007 [DIRS 177404]) have also been developed. Investigations with the homogeneous drift-scale THC seepage model (SNL 2007 [DIRS 177404]) provided estimates of THC changes in the near-field rock and chemistry of likely seepage water. However, they did not report any seepage into the drifts because of the absence of heterogeneities in fracture permeability and capillarity (which are key parameters controlling seepage; see Sections 6.1.2) in the homogeneous drift-scale THC seepage model (SNL 2007 [DIRS 177404]). Thus, for the sake of consistency, there is a need to integrate some aspects of the seepage calibration model (SCM) and the SMPA model into the drift-scale THC seepage model. This is what is accomplished in the present report.

6.3 IMPACT OF THC PROCESSES ON SEEPAGE

When liquid water, having flowed through the unsaturated rock, reaches the immediate vicinity of an emplacement drift, a layer of increased saturation is expected to develop as a result of the capillary-barrier effect from the drift opening (Philip et al. 1989 [DIRS 105743]; Jackson et al. 2000 [DIRS 141523]; Finsterle 2000 [DIRS 151875]; Finsterle et al. 2003 [DIRS 163214]). Water is prevented from seeping into the drift because of capillary suction, which retains the wetting fluid in the pore space of the rock. This barrier effect leads to a local saturation buildup in the rock next to the interface between the geologic formation and the drift. If the permeability (as well as the capillarity) of the fracture network within this layer is sufficiently high, all or a portion of the water is diverted around the drift under partially saturated conditions. Locally, however, the water potential in the formation may be higher than that in the drift, and then water exits the formation and enters the drifts, resulting in seepage.

In the unsaturated fractured rock of Yucca Mountain, the fractures form a well-connected network. As a result, flow is mostly carried in the fractures. Moreover, because the permeability of the rock matrix is a few orders of magnitude smaller than that of the fracture network, flow in the rock matrix is considerably slower. In addition, the smaller pores of the rock matrix ensured a stronger capillary suction compared to the fractures. Thus, the matrix mainly provides storage, while flow takes place through the fractures. The potential for seepage from the matrix is thus significantly smaller than from the fractures. The formulation that follows is therefore focused on the flow in fractures.

Earlier studies (Jackson et al. 2000 [DIRS 141523]; Or and Ghezzehei 2000 [DIRS 144773]; Finsterle 2000 [DIRS 151875]; Finsterle et al. 2003 [DIRS 163214]; BSC 2004 [DIRS 171764]) have shown that a heterogeneous porous continuum representation can be consistently used to analyze flow in unsaturated fractured rock, particularly if the fractures are rough-walled or are partially filled. For analyzing the impact of THC processes on seepage, the same fundamental approach is adopted in this report. As an example, the mechanism of seepage into an emplacement drift is schematically shown in Figure 6.3-1. In that figure, flow is shown to be

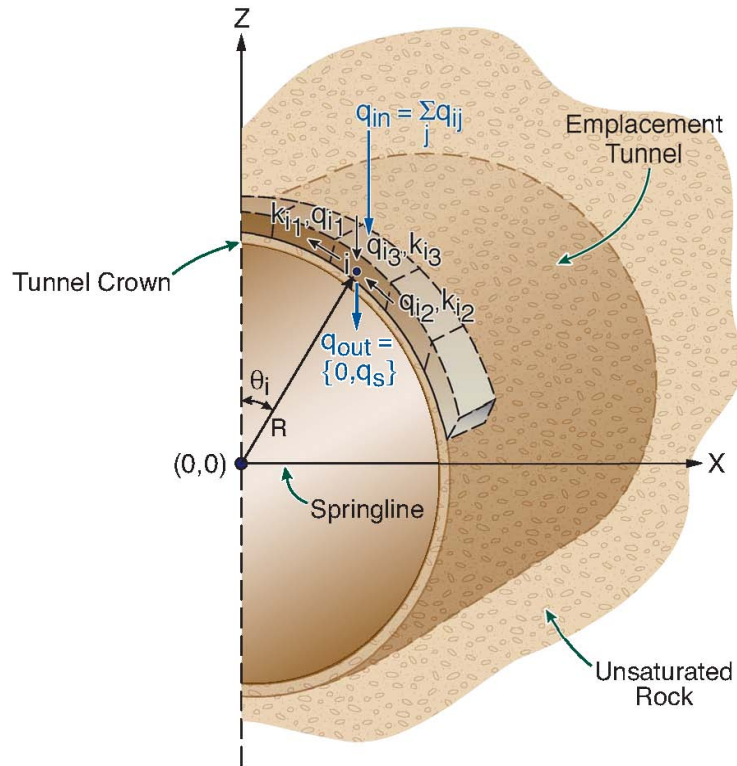


Figure 6.3-1. Schematic Representation of Seepage into an Emplacement Drift Situated in Unsaturated Fractured Rock

On the other hand, if the above condition is not satisfied (i.e., if the net flow of water into the block is less than the seepage flux), the saturation in rock block i will decrease (and fall below the threshold saturation over time), the capillary suction of the rock will increase, and seepage will stop.

It has already been shown (Equation 6.3-4) that seepage can take place only when the capillary suction of the fractures is smaller than the gravitational forces. Since the capillary pressure is a function of liquid saturation, Equation 6.3-4 can be rewritten as

$$\frac{1}{\alpha_i} F(S_i^l) \leq \rho g h \quad (\text{Eq. 6.3-6})$$

where $(1/\alpha_i)$ is the fracture capillary-strength parameter of block i and $(1/\alpha_i)F(S_i^l)$ represents the dependence of fracture capillary pressure on liquid saturation (S_i^l). It is also known that the fracture $(1/\alpha_i)$ parameter changes with fracture porosity (φ_i) and permeability (k_i) of block i through Leverett scaling (Leverett 1941 [DIRS 100588]) as

$$\frac{1}{\alpha_i} = \frac{1}{\alpha_0} \sqrt{\frac{k_0 \varphi_i}{k_i \varphi_0}} \quad (\text{Eq. 6.3-7})$$

3. A 2-D representation of THC processes does not account for the axial transport of vapor and air along the open drifts, a result of natural convection processes and gas pressure differences along the drifts. As demonstrated in *In-Drift Natural Convection and Condensation* (BSC 2004 [DIRS 164327]), such processes can effectively move water vapor from the heated emplacement sections of the drifts to the cooler rock surfaces at the drift ends outside of the emplacement sections (turn-out sections). Principles of thermodynamics suggest that the maximum amount of vapor that can be present in an air-vapor mixture decreases with declining temperature. Thus, the warm moist gas moving from hot waste packages into the comparably cool turnouts will be depleted of most of its vapor content by condensation on cooler rock surfaces. At the same time, relatively dry gas circulates back towards the emplacement sections of the drifts, thereby reducing the vapor mass and the relative humidities in these heated areas. Thus, a 2-D representation—that does not account for axial vapor transport along drifts—is likely to overestimate the amount of vapor in the near-field rock mass in all heated drift sections, i.e., in those drift sections that are most relevant for thermal seepage and the related abstraction model. Overestimating the humidity in the drift leads to underestimation of evaporation, and thus overestimation of seepage. Thus, a 2-D representation without accounting for in-drift vapor flux is an upper-bounding case for seepage.
4. A 2-D representation does not capture the three-dimensional behavior of small-scale flow channeling in the fractured rock, as caused by heterogeneity in the rock properties. However, with respect to the effectiveness of the capillary-barrier for seepage into drifts, a 2-D representation is more critical in most cases of heterogeneous fracture permeability fields, because the potential diversion of flow in the third dimension is neglected (Hardin et al. 1998 [DIRS 100350], Section 3.6).

It can be concluded from the itemized list that the 2-D representation used in this report is adequate for the intended application of predicting seepage.

6.4.2 2-D Model Domain

Simulations were performed in a 2-D vertical cross section through the unsaturated fractured rock at Yucca Mountain, using the numerical grid shown in Figure 6.4-1. The source of this model domain is DTN: LB0705DSTHC001.002 [DIRS 180854] (folder: \thc7_81_w0_, file: “MESH”), which is included in Table 4.1-1 as a direct input. Since thermal perturbation from repository heating is expected to occur over tens of meters above and below an emplacement drift (see Section 6.6.1), the vertical model domain comprises the entire unsaturated zone at Yucca Mountain (the model domain extends approximately 364 m above and approximately 353 m below an emplacement drift). Such an approach ensures proper implementation of boundary conditions (see Sections 6.4.3 and 6.6.1). The model domain extends 40.5 m laterally (or in the horizontal direction), extending from the center of one emplacement drift to the mid-point between two drifts. Both vertical boundaries are treated as no-flow boundaries. Symmetry is assumed with the symmetry plane parallel to the drift axis. The grid is radial (owing to the cylindrical geometry of the emplacement drift) and refined (with gridblocks as small as 0.2 m) in the vicinity of the drift, but coarser farther away from the drifts, gradually transforming into a rectangular grid. Drift radius is 2.75 m, and the model domain has a thickness of 1 m.

investigated with the THC seepage model to cover the range of variability in the infiltration fluxes within the repository horizon. These include applying ten times the IMF1 fluxes. These simulations will be referred to as IMF10.

6.4.6 Rock Hydrological and Thermal Properties

Rock hydrological and thermal properties are obtained from DTN: LB0705DSTHC001.002 [DIRS 180854]; Table 4.1-1 provides information about where the rock hydrological and thermal properties can be found in that DTN. Except for the fracture $1/\alpha$ parameter of the Tptpl unit (which is considered a sensitivity parameter), the calibrated matrix and fracture hydrological properties used in this report correspond to the 30th percentile parameter set as given in *Calibrated Unsaturated Zone Properties* (SNL 2007 [DIRS 179545], Table 6-7). More details about the thermal and hydrological properties can be found in *Drift-Scale THC Seepage Model* (SNL 2007 [DIRS 177404], Sections 4.1.1 and 6.4.7). Most of the layer-averaged hydrologic properties are based on calibration against borehole measurements such as saturation data, water-potential data, pneumatic pressure data, and ambient temperature data. For convenience, a summary of the key thermal and hydrological properties for the repository units (the host rock for the emplacement drifts) is provided in Table 6.4-2, which is reproduced from *Drift-Scale THC Seepage Model* (SNL 2007 [DIRS 177404], Table 6.4-2).

Table 6.4-2. Summary of Hydrological and Thermal Properties of Repository Units

Geological Unit>		30th Percentile Parameter Set		
		Tptpul (tsw33)	Tptpmn (tsw34)	Tptpll (tsw35)
MATRIX DATA				
Permeability	k_m (m ²)	1.86E-17	3.16E-18	1.11E-17
Porosity	f_m (-)	0.155	0.111	0.131
van Genuchten α	α_m (1/Pa)	6.56E-6	1.71E-6	3.38E-6
van Genuchten m (or λ)	m_m (-)	0.283	0.317	0.216
Residual saturation	S_{lrm} (-)	0.12	0.19	0.12
Rock grain density	ρ (kg/m ³)	2,520	2,520	2,540
Rock grain specific heat capacity	C_p (J/kg K)	930	930	930
Dry thermal conductivity	λ_{dry} (W/m/K)	1.22	1.39	1.24
Wet thermal conductivity	λ_{wet} (W/m/K)	1.78	2.06	1.87
Tortuosity	τ (-)	0.20	0.20	0.20
FRACTURE DATA				
Permeability	k_f (m ²)	7.8E-13	3.3E-13	9.1E-13
Porosity	f_f (-)	5.8E-3	8.5E-3	9.6E-3
van Genuchten α	α_f (1/Pa)	1.58E-3	3.16E-4	5.75E-4
van Genuchten m (or λ)	m_f (-)	0.633	0.633	0.633
Residual saturation	S_{lrf} (-)	0.01	0.01	0.01

Table 6.4-6. Intermediate-Scale Variability Statistics of Estimated Capillary-Strength Parameter over Repository Rock Block, Using Different Calculation Methods

Method	Number of Samples	Mean μ (Pa)	Std. Dev. σ (Pa)	Std. Error (Std. Dev. of Mean) (Pa)
A: All Samples, Both Units	10	591	109	35
B: All Locations, Both Units	4	631	109	54
C: All Samples in Tptpmn All Samples in Tptpll	4 6	604 582	131 105	66 43
D: All Locations in Tptpmn All Locations in Tptpll	2 2	650 613	129 132	91 93

Source: DTN: LB0407AMRU0120.001 [DIRS 173280]; also given in BSC 2004 [DIRS 169131], Table 6.6-2. Inside the DTN, go to folder \capillary_strength_analysis and locate the file capillary_strength_summary_tables.doc for the values reported in this table.

6.4.11.2 Dimensionality and Scale

The fracture capillary-strength parameters in *Seepage Calibration Model and Seepage Testing Data* (BSC 2004 [DIRS 171764], Section 6) were obtained by calibrating to liquid-release test data based on the following conceptualizations:

- 3-D flow fields
- Applicable to only small-scale fracture flow close to the emplacement drifts
- Heterogeneities in fracture permeability have no impact on calibrated fracture capillary-strength parameters.

In previous thermal seepage studies (BSC 2005 [DIRS 172262]; BSC 2006 [DIRS 174104]), even though the conceptual model was 2-D, the calibrated fracture capillary-strength parameter (which was obtained through 3-D calibration) from *Seepage Calibration Model and Seepage Testing Data* (BSC 2004 [DIRS 171764]) was used. In addition, even though the calibrated fracture capillary-strength parameter was representative of a small zone close to the emplacement drift, it was adopted for the fracture continuum of the entire Tptpll (or tsw35) unit. Because the objective in the two earlier reports (BSC 2005 [DIRS 172262]; BSC 2006 [DIRS 174104]) was to use a conservative approach with respect to seepage (i.e., simulate conditions that were most favorable for seepage), it was appropriate to adopt the calibrated fracture capillary-strength parameter on the following grounds:

- If a 2-D conceptual model were to be used in calibrating the liquid-release test data, it would have resulted in a larger estimated fracture capillary-strength parameter for the host rock Tptpll (see Section 6.4.11.3). A larger fracture capillary-strength parameter for Tptpll would have resulted in prediction of less seepage. Therefore, using a smaller fracture capillary-strength parameter was justified, since it was conservative.

- The SCM calibrated fracture capillary-strength parameter value represents conditions close to an emplacement drift. However, the SCM calibrated fracture-capillary strength parameter value was used for the entire host rock, T_{ptpl} . Applying the SCM calibrated fracture capillary-strength parameter value for the entire fracture continuum of T_{ptpl} implied that the fractures in general had smaller water retention ability (because the SCM calibrated fracture capillary-strength parameter value was much smaller than the T_{ptpl} value). This, again, created situations favorable for water entering an emplacement drift rather than staying in the rock. In other words, this approach provided conservative results with respect to seepage.

6.4.11.3 Leverett-Scaling Effects

While the approach adopted in earlier seepage studies (BSC 2005 [DIRS 172262]; BSC 2006 [DIRS 174104]) was justified on the basis of dimensionality and scale as discussed above, one issue that was not addressed in those reports was the impact of permeability heterogeneity on fracture capillarity. Further evaluation of the calibration process is needed to account for the Leverett-scaling effects.

The prediction of seepage under ambient conditions is based on an approach that uses a suite of consistent models: (1) seepage-relevant, model-related parameters are estimated by calibrating a numerical model to seepage data from liquid-release tests conducted in various niches and the ECRB (BSC 2004 [DIRS 171764]); (2) a conceptually consistent prediction model is used to examine seepage into waste emplacement drifts for many seepage-relevant parameter combinations (BSC 2004 [DIRS 167652]); and (3) a seepage abstraction model is developed that determines probability distributions for these seepage-relevant parameters, accounting for spatial variability and uncertainty, and incorporating other effects (BSC 2004 [DIRS 169131]). Since the calibration process yields parameters that can be considered optimal for the given process, scale, and model structure, it is essential that the prediction model be conceptually consistent with the calibration model to minimize the risk of introducing a potential bias. Thus, since the calibration (BSC 2004 [DIRS 171764]) was performed with homogeneous capillarity (i.e., Leverett scaling was excluded), the SMPA (BSC 2004 [DIRS 167652]) and the seepage abstraction model (BSC 2004 [DIRS 169131]) also did not include the Leverett-scaling effects for the sake of consistency.

However, if the conceptual model (which includes governing equations, treatment of heterogeneity, model dimensionality, and discretization) is changed, the model parameters will need to be adjusted accordingly. Specifically, it is expected that the reference van Genuchten capillary-strength parameter $1/\alpha$ (determined using the three-dimensional calibration model with a heterogeneous permeability field but with homogeneous capillary-strength) needs to be changed if used in a predictive model in which the small-scale capillary-strength is correlated to the heterogeneous permeability field using the Leverett-scaling rule (Equation 6.3-7).

A synthetic inversion study is performed to examine the potential adjustment that needs to be made to the capillary-strength parameter when changing the conceptual model for SCM (i.e., by adding Leverett-scaling effects). Synthetic seepage data are generated by simulating a liquid-release test using a conceptual model similar to that used for the calibration of actual liquid-release test data, i.e., a three-dimensional, heterogeneous model with a uniform

initial fracture capillary-strength parameter is used in all base-case simulations irrespective of whether Leverett scaling is included, the capillary-barrier effects imposed by a base-case simulation including Leverett scaling is different from a base-case simulation excluding Leverett scaling.) Additional sensitivity simulations (by changing the initial fracture capillary-strength parameters) were thereafter performed with the THC seepage model (SNL 2007 [DIRS 177404]) by changing the initial fracture capillary-strength parameter.

The choice of the initial fracture capillary-strength parameters for these additional sensitivity simulations depended on whether Leverett-scaling effects were excluded. When Leverett-scaling effects were excluded, the initial fracture capillary-strength parameter was adopted from the SCM (BSC 2004 [DIRS 171764]), since this presented a conservative approach for seepage. (The calibrated fracture capillary-strength parameter was obtained using a 3-D conceptual model but was used in a 2-D predictive model, lowering the capillary-barrier effects and increasing the potential for seepage.) These simulations are discussed in Section 6.7.1.

When Leverett-scaling effects are included, the choice of the initial fracture capillary-strength parameter is somewhat more complicated. Section 6.4.11.3 provides some guidelines; however, no direct calibrated fracture capillary-strength parameters are available for these simulations (the SCM cannot be used because it does not include Leverett scaling). An iterative scheme is therefore used to determine the initial fracture capillary-strength parameter, which will provide approximately the maximum potential for seepage (by adopting a fracture capillary-strength parameter that approximately provides a minimum of the capillary-barrier effects). These iterative simulations are described in Section 6.7.2.1, and seepage results from them can be found in Section 6.7.2.2.

6.5.1 Non-Convergent Simulations

One of the THC simulations (Simulation ID “base_r1_10x_lev_thc” in Table 6.5-2) was not completed. This simulation did not continue beyond 2,000 years because of numerical difficulties and was abandoned. The numerical difficulty encountered by this simulation is specific to this simulation only, and has no impact on other simulations in this report. Recollect that different realizations of the same fracture permeability distribution are used in this report. For this particular simulation with Realization # 1 of the permeability distribution, the initial permeability of a few gridblocks and their spatial/temporal evolution were such that it resulted in a singular matrix in the chemical solver routine of the software TOUGHREACT. Thus, non-convergence for this simulation was not because of any coding or data-entry error, but because of a rare occurrence. Since results from a large number of simulations are available (see also Sections 6.6 and 6.7) satisfying the requirements of this THC sensitivity report, completion of this particular simulation is not considered essential. Also, because the simulation was not completed after 2,000 years, results from this simulation up to 2,000 years have not been submitted to the TDMS and have not been used in reaching any conclusion.

From Figure 6.6-1, it can be seen that temperatures are well above boiling near the emplacement drift. On the other hand, temperatures are close to ambient conditions beyond approximately 80 m above and below the emplacement drift. In other words, the thermal perturbation does not extend beyond 80 m above and below the emplacement drift for this particular simulation. Since temperatures are near maximum at 100 years after emplacement of waste packages (recall also that ventilation is turned off 50 years after emplacement of wastes), this possibly represents the maximum limits of the spatial extent of thermal perturbation. Though not shown here, temperature contours from the other base-case simulations are similar. In short, since the top and bottom boundaries are located at 364 m above and 353 m below the emplacement drift, respectively, it is reasonable to conclude that thermal perturbations do not reach the top and bottom boundaries of the THC seepage model domain. Thus, the constant temperature boundaries at the top and bottom of the THC seepage model domain have no significant impact on the evolution of temperatures in the host rock.

6.6.2 Seepage Rates

From Table 6.5-2, it can be seen that 36 base-case simulations were performed with the THC seepage model (though one of them could not be completed, see Section 6.5.1). These include simulations with three realizations of the heterogeneous fracture permeability distribution and two infiltration fluxes (IMF1 and IMF10). The simulations were performed with and without Leverett-scaling effects. All these combinations were repeated for ambient, TH, and THC simulations. The purpose of the base-case simulations was to analyze the sensitivity of the THC seepage model to permeability heterogeneity and infiltration fluxes, while keeping the initial fracture capillary-strength parameter for the Tptpl unit constant. Impact of capillarity heterogeneity can be observed by comparing the results from simulations with Leverett-scaling effects (capillarity is heterogeneous through Equation 6.3-7) and without those effects (capillarity is homogeneous). Thus, the base-case simulations cover a range of permeability and capillarity heterogeneity for a given initial fracture capillary-strength parameter (see Section 6.4.11).

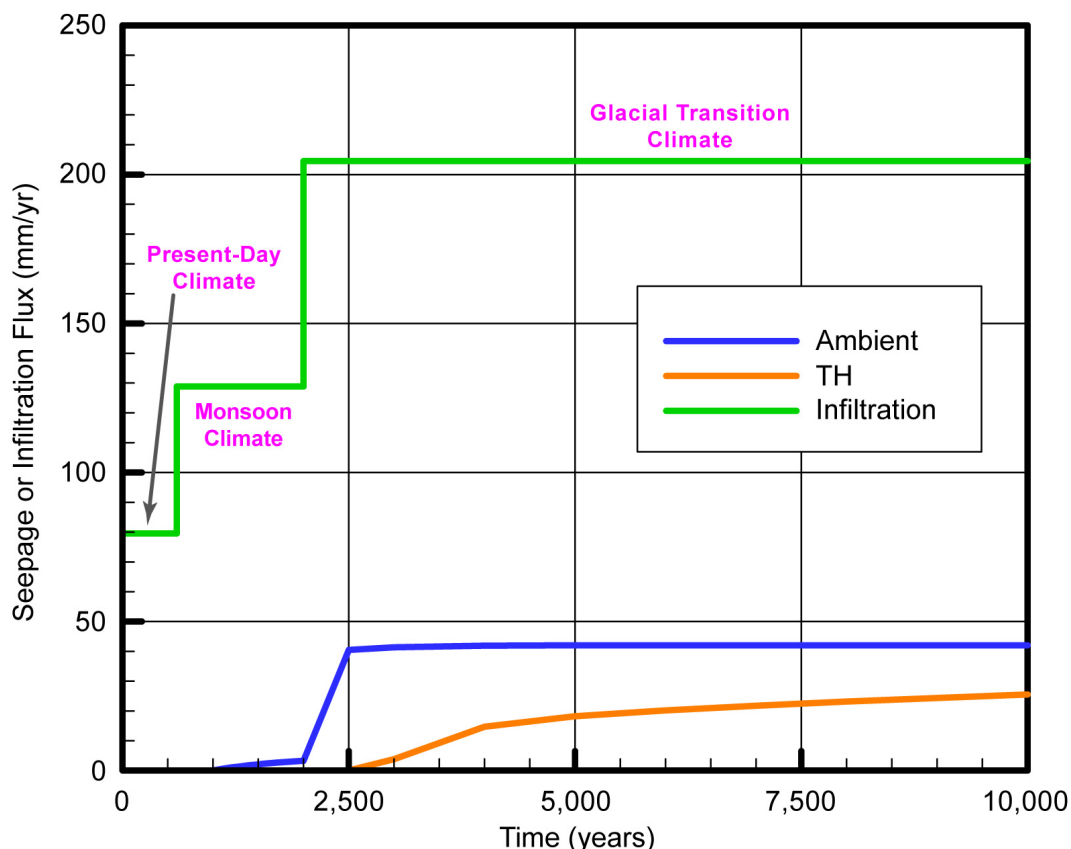
Seepage results (whether seepage happens or not) from the base-case simulations are tabulated in Table 6.6-1. These results have been submitted to the TDMS; the output DTN for each of the 36 base-case simulations is also included in Table 6.6-1 (see also Table 6.5-2). The seepage results can be extracted from files “flow.out” in the output DTNs. Appendix D describes the procedures for how to extract the seepage results from the “flow.out” files.

A few observations can be made from the results summarized in Table 6.6-1.

- No seepage is observed for any of the three realizations of the heterogeneous fracture permeability distribution with IMF1 infiltration fluxes (see Section 6.4.5), if *Leverett-scaling effects are ignored*. This is true even with IMF10 (ten times the IMF1 fluxes; see Section 6.4.5) infiltration fluxes. This is also true whether ambient, TH, or THC simulations are considered.

The initial fracture capillary-strength parameter ($1/\alpha_0$) for the Tptpl unit in these base-case simulations is 1,739 Pa. If capillarity is assumed spatially uniform and independent of permeability (i.e., Leverett scaling is ignored), for the Tptpl fracture properties provided in Table 6.4-2, the seepage threshold saturation (Equation 6.3-10) is quite large (~ 0.8196). In other words, a fracture element just outside the emplacement drift must have a saturation of 0.8196 or larger for seepage to occur. The results show that this condition was not satisfied in any of the simulations, and consequently, seepage is not predicted from these simulations. This implies that the capillary-barrier effect is too strong and excludes flow from entering the drift in these simulations.

- When fracture capillarity is correlated to fracture permeability/porosity heterogeneity (i.e., *Leverett-scaling effects are included*), using the IMF1 fluxes, no seepage is predicted in TH or THC simulations with any of the realizations of the heterogeneous permeability distributions. Ambient simulations also predict no seepage for two of the realizations of the permeability distribution (Realization #1 and Realization #3). However, minor seepage (approximately 1.66 mm/yr or approximately 8.12% of the infiltration fluxes) is predicted in ambient simulation with Realization #2 (Simulation ID: “base_r2_1x_lev_amb”; see Tables 6.5-2 and 6.6-1). This particular simulation predicts seepage to occur after 2,000 years.
- When IMF10 (see Section 6.4.5) infiltration fluxes are used and Leverett-scaling effects are included, seepage is predicted to occur from both ambient and TH simulations with Realization #1 (Simulation IDs: “base_r1_10x_lev_amb” and “base_r1_10x_lev_th”; see Table 6.5-2). Note that results from the corresponding THC simulation (Simulation ID: “base_r1_10x_lev_thc”) are not available (see Tables 6.5-2 and 6.6-1), as explained in Section 6.5.1.. Figure 6.6-2 compares the seepage fluxes from simulations “base_r1_10x_lev_amb” and “base_r1_10x_lev_th.” Note that the ambient seepage fluxes are larger than seepage from TH simulations. Figure 6.6-2 also shows the infiltration fluxes for IMF10 scenario (see Section 6.4.5) and the different climate periods (present-day, monsoon, and glacial transition; see Section 6.4.5). Maximum seepage flux from these simulations is predicted to be less than 21% (ambient simulations) and 13% (TH simulations). Predicted TH seepage fluxes are less than ambient seepage fluxes because of the vaporization barrier effect created by the repository thermal load (see Sections 6.1.1 and 6.1.2). Note that the seepage percentages are calculated based on the maximum infiltration fluxes (i.e., ten times the infiltration fluxes of the glacial transition period).

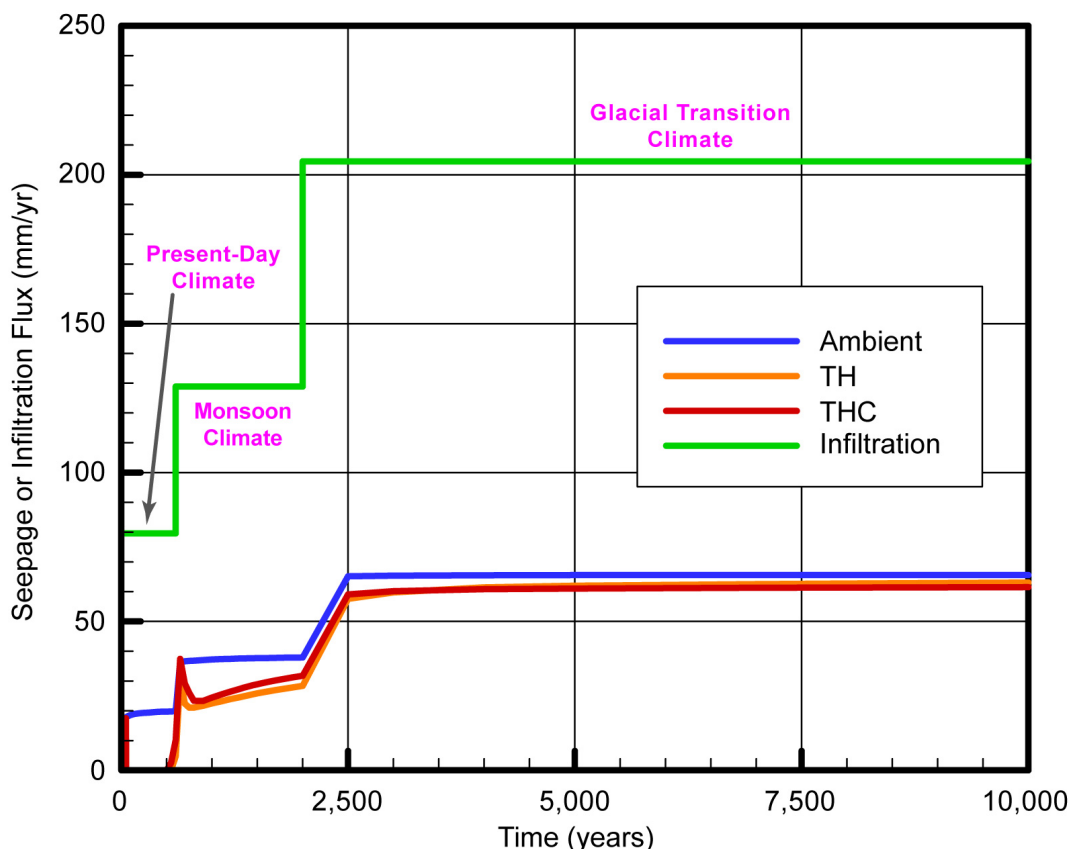


Source: Output DTNs: LB0705THCSEN1.002 and LB0705THCSEN1.003.

NOTE: See Table 6.5-2 for explanation of simulation IDs. The corresponding THC simulation (Simulation ID: "base_r1_10x_lev_thc") could not be completed (see Table 6.6-1).

Figure 6.6-2. Comparison of Seepage Fluxes from Ambient (Simulation ID: "base_r1_10x_lev_amb") and TH (Simulation ID: "base_r1_10x_lev_th") Simulations with IMF10 Infiltration Fluxes

For corresponding ambient, TH, and THC simulations with Realization #2 (Simulation IDs: "base_r2_10x_lev_amb," "base_r2_10x_lev_th," and "base_r2_10x_lev_thc"), seepage is predicted by all of them. Figure 6.6-3 compares the seepage fluxes from these three simulations for Realization #2. Ambient seepage fluxes are again predicted to be larger than both TH and THC seepage. The predicted pattern of seepage from these three simulations illustrates the dynamic nature of the underlying processes. For this realization of the heterogeneous permeability distribution (in combination with the initial fracture capillary-strength parameter of 1,739 Pa), ambient simulations predict seepage at all times (as confirmed by even the ambient simulation with IMF1 infiltration fluxes; see Simulation ID "base_r2_1x_lev_amb" in Tables 6.5-2 and 6.6-1). TH and THC simulations also predict small amounts of seepage at the beginning (between 0 and 50 years) and no seepage immediately after ventilation stops (as the host rock heats through the boiling temperatures). In TH and THC simulations, seepage returns after the boiling period is over and temperatures have dropped below boiling. Overall, the predicted patterns of seepage from TH and THC simulations are similar (with ambient seepage being marginally larger than the other two). Maximum seepage flux is approximately 32% of the infiltration fluxes.



Source: Output DTNs: LB0705THCSEN2.001, LB0705THCSEN2.002, and LB0705THCSEN2.003.

NOTE: See Table 6.5-2 for explanation of simulation IDs.

Figure 6.6-3. Comparison of Seepage Fluxes from Ambient (Simulation ID: “base_r2_10x_lev_amb”), TH (Simulation ID “base_r2_10x_lev_th.”), and THC (Simulation ID: “base-r2_10x_lev_thc”) Simulations with IMF10 Infiltration Fluxes

Thus, the combination of Realization #2 of the heterogeneous permeability distribution and an initial fracture capillary-strength parameter of 1,739 Pa did not provide a strong enough capillary-barrier effect to prevent even ambient seepage. Since fracture capillarity (and consequently, capillary-barrier effect) is in this case a local phenomenon because of the formulation of Leverett scaling (Equation 6.3-7), these results highlight the local nature of the process.

This result is further confirmed by the corresponding simulation results with Realization #3 of the heterogeneous fracture permeability distribution. In this case, none of the ambient (Simulation ID: “base_r3_10x_lev_amb”), TH (Simulation ID: “base_r3_10x_lev_th”), and THC (Simulation ID: “base_r3_10x_lev_thc”) simulations show any seepage. This implies that, for this realization of the fracture permeability distribution in combination with an initial fracture capillary-strength parameter, the local capillary-barrier effect is too strong.

- The base-case simulations demonstrate the impact of fracture permeability and capillarity heterogeneity on seepage. When fracture permeability heterogeneity is included in the conceptual model and capillarity is assumed homogeneous (i.e., Leverett scaling is not

included), the selected fracture capillary-strength parameter (1,739 Pa) resulted in a large seepage threshold saturation (~0.8196), which did not allow seepage to occur with either the IMF1 infiltration fluxes or the IMF10 infiltration fluxes. However, with inclusion of both permeability and capillarity heterogeneity in the conceptual model through Leverett scaling, local situations are created in which the seepage threshold saturations are considerably smaller (i.e., locations with considerably larger permeability than the mean fracture permeability). This is demonstrated in Table 6.6-2 where the impact of permeability heterogeneity (keeping porosity constant) on seepage threshold saturation is demonstrated for the fracture properties provided in Table 6.4-2. Observe that, if the permeability is two orders of magnitude larger than the mean fracture permeability, seepage threshold saturation decreases to approximately 0.017 (it is ~0.8196 when capillarity is uniform). Such a local decrease in seepage-threshold saturation makes seepage possible when capillarity heterogeneities are included in model conceptualization, particularly when enhanced infiltration fluxes are imposed.

Table 6.6-2. Example Calculations Showing Impact of Permeability Heterogeneity on Seepage Threshold Saturation through Leverett Scaling (Equations 6.3-7 and 6.3-10)

Item Number	Mean Fracture Permeability (m ²)	Local Gridblock Fracture Permeability (m ²)	Leverett Factor ^a (Equation 6.3-7) (-)	Seepage Threshold Saturation ^b (Equation 6.3-10) (-)
1.	0.91×10^{-12}	0.91×10^{-14}	0.1000	0.9996
2.	0.91×10^{-12}	0.91×10^{-13}	0.3162	0.9906
3.	0.91×10^{-12}	0.91×10^{-12}	1.0000	0.8196
4.	0.91×10^{-12}	0.91×10^{-11}	3.1622	0.1638
5.	0.91×10^{-12}	0.91×10^{-10}	10.0000	0.0168

^a Porosity is assumed to be equal to mean fracture porosity. Leverett factor is calculated as the square root of the ratio of local gridblock fracture permeability and mean fracture permeability.

^b For these seepage threshold calculations using Equation 6.3-10, water density ρ is 1,000 kg/m³; h is 0.1 m (the distance of the center of the gridblock from the drift wall); and g (acceleration due to gravity) is 9.81 m/s²; α_0 is 1,739 Pa; m is 0.6330; γ is 0.4000; and S_{lr} is 0.01. For the source of the parameters α_0 , m , γ , and S_{lr} , see Table 6.4-2.

- For the base-case simulations in which seepage happens, Table 6.6-3 provides the maximum seepage percentage (as a percentage of the imposed infiltration fluxes). Table 6.6-3 also identifies the simulation type (ambient, TH, or THC) from which maximum seepage happens. Observe that, when seepage happens (particularly for greater imposed infiltration fluxes), ambient seepage is always larger than TH or THC simulations. This is important because it implies that seepage abstraction can continue to be based on ambient seepage rates (i.e., THC processes provide no enhancement in seepage).
- The other important conclusion is that, even though the initial fracture capillary-strength parameter was the same between simulations excluding and including Leverett-scaling

effects, the capillary-barrier effects computed by them were not the same. As the |
discussion in

The time-profiles of distance from drift center, temperature, and liquid saturation for model gridblocks representing TOP FLUX waters are shown in Figures 6.6-4 to 6.6-6. These profiles provide a context for the chemistry profiles discussed afterwards. For simulated times up to 50 years, TOP FLUX waters represent gridblocks directly above, and adjacent to, the drift crown (i.e., at a distance ~ 2.8 m from drift center) (Figure 6.6-4). From the onset of boiling at approximately 50 years, the TOP FLUX waters correspond to the condensation/reflux zone in fractures directly above the boiling front, and thus their distance from drift center corresponds approximately to the extent of dryout zone in fractures (Figures 6.6-4 and 6.6-5). For the IMF1 infiltration scenario, these distances drop down to ~ 2.8 m at the same time drift-wall temperature drops down below $\sim 96^\circ\text{C}$ (Figure 6.6-5), the boiling point for the modeled elevation. This behavior indicates that the rewetting front in fractures around the drift more or less coincides with the collapse of the boiling front, with rewetting of the drift wall occurring at about 1,300 years. For the IMF10 infiltration scenario, the boiling front collapses earlier (at about 400 years), and boiling continues at the drift wall for several hundred years (Figures 6.6-4 and 6.6-5).

The spatial variability in liquid saturation for gridblocks located in the condensation/reflux zone typically translates directly to the variability of predicted concentrations of dissolved species in that zone. This is because variations in liquid saturation caused by dilution and evaporation directly affect concentrations. For each model run, predicted liquid saturations at TOP FLUX locations with highest liquid mobility (INDX=1) show trends of higher saturation with higher infiltration, as well as higher saturations in the heterogeneous (versus homogeneous) case (Figure 6.6-6).

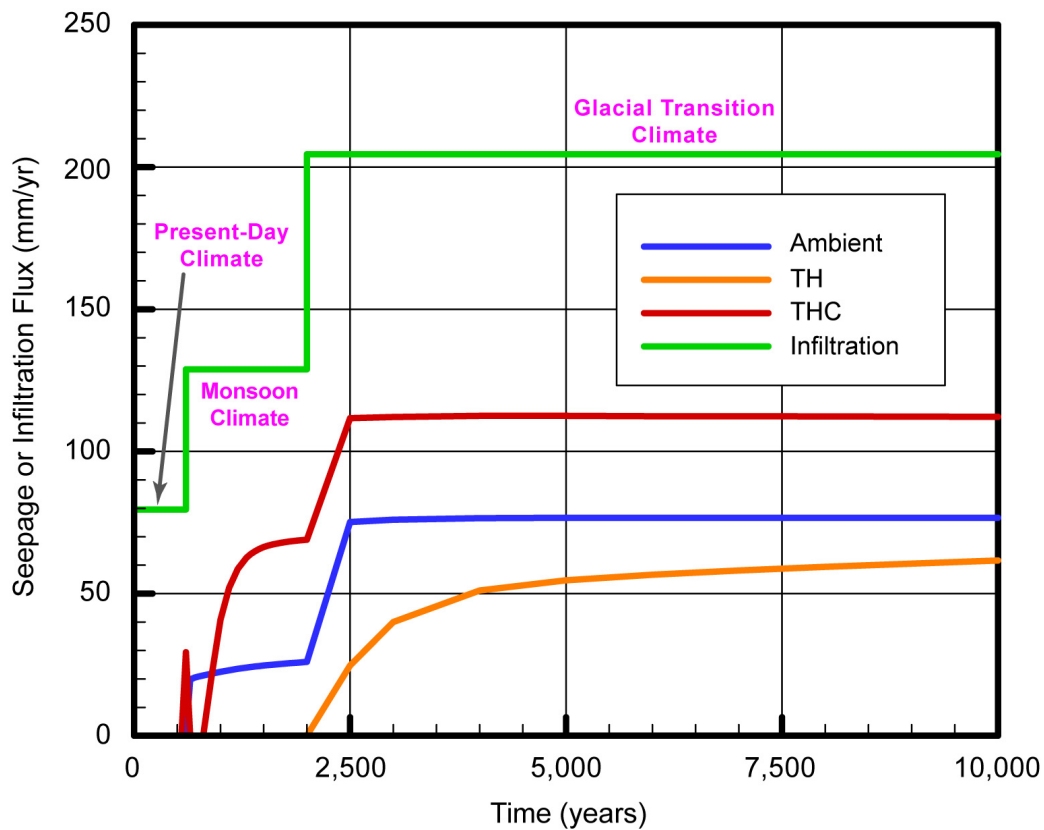
Predicted profiles of concentration versus time for CO_2 gas and aqueous species of interest are shown in Figures 6.6-7 through 6.6-17. Details on processes affecting these concentration trends (evaporation, dilution, water-rock interactions) are discussed in *Drift-Scale THC Seepage Model* (SNL 2007 [DIRS 177404], Section 6.5.5.4) and not repeated here.

Several important observations can be made from these figures. The main observation is that for the IMF1 infiltration scenario, predicted concentration profiles of aqueous species with heterogeneous and homogeneous permeability fields do not differ significantly. In fact, when the full spread in results is taken into account (i.e., when considering data for gridblocks with attribute INDX = 1 through 6, instead of only 1, as shown in Figures 6.6-7 through 6.6-17), the profiles for both cases essentially overlap. This is consistent with conclusions from earlier work (BSC 2004 [DIRS 168848], Section 6.6) asserting that fracture permeability heterogeneity would not significantly affect predicted water compositions. This is because the host-rock mineralogical composition around drifts is fairly homogeneous, even though the permeability of these rocks is not. Since the predicted seepage chemistries from heterogeneous simulations are expected to be similar to those from homogeneous simulations (as evidenced by the results and discussion in this section), analyses of seepage water from other heterogeneous simulations are not included in this report.

Another observation from Figures 6.6-7 through 6.6-17 is that the character of in-drift water evolves, with time, from dilute, mildly acidic compositions representing in-drift condensation, to compositions representative of waters in rocks near the drift wall (e.g., Figures 6.6-7 and 6.6-9). Discarding initial effects of condensation, these results are consistent with earlier assertions that

From Table 6.7-2, it can be seen that seepage is not predicted to occur for any of the three realizations of heterogeneous fracture permeability distribution, if IMF1 infiltration fluxes are imposed. This is true for THC simulations as well as ambient and TH simulations. In other words, for the IMF1 infiltration fluxes (7.96 mm/yr for 0 to 600 years, 12.45 mm/yr for 600 to 2,000 years, and 20.45 mm/yr for 2,000 years and beyond), the saturation buildup near the emplacement drift is not sufficient to overcome the capillary-barrier effect created by a fracture capillary-strength parameter of 591 Pa (the seepage threshold saturation, ignoring Leverett-scaling effects, when the initial fracture capillary-strength parameter 591 Pa, is approximately 0.1921).

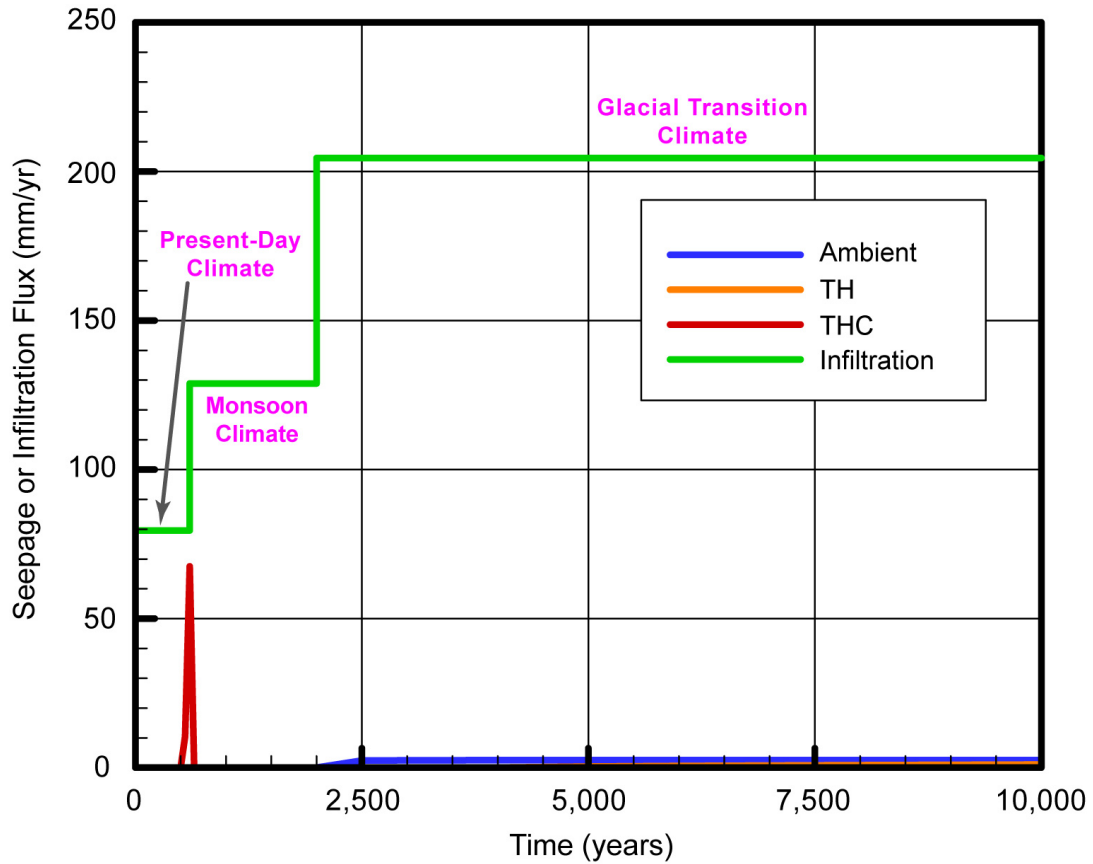
When IMF10 infiltration fluxes (79.6 mm/yr for 0 to 600 years, 128.9 mm/yr for 600 to 2,000 years, and 204.5 mm/yr for 2,000 years and beyond) are imposed on the THC seepage model (SNL 2007 [DIRS 177404]), the saturation buildup at certain locations on the drift wall does exceed the seepage saturation threshold of approximately 0.1921, leading to occurrence of seepage. Figures 6.7-1, 6.7-2, and 6.7-3 show the seepage flux (in mm/yr) from Realizations #1, #2, and #3, respectively.



Source: Output DTNs: LB0705THCSEN1.004, LB0705THCSEN1.005, and LB0705THCSEN1.006.

NOTE: See Table 6.7-1 for explanation of simulation IDs.

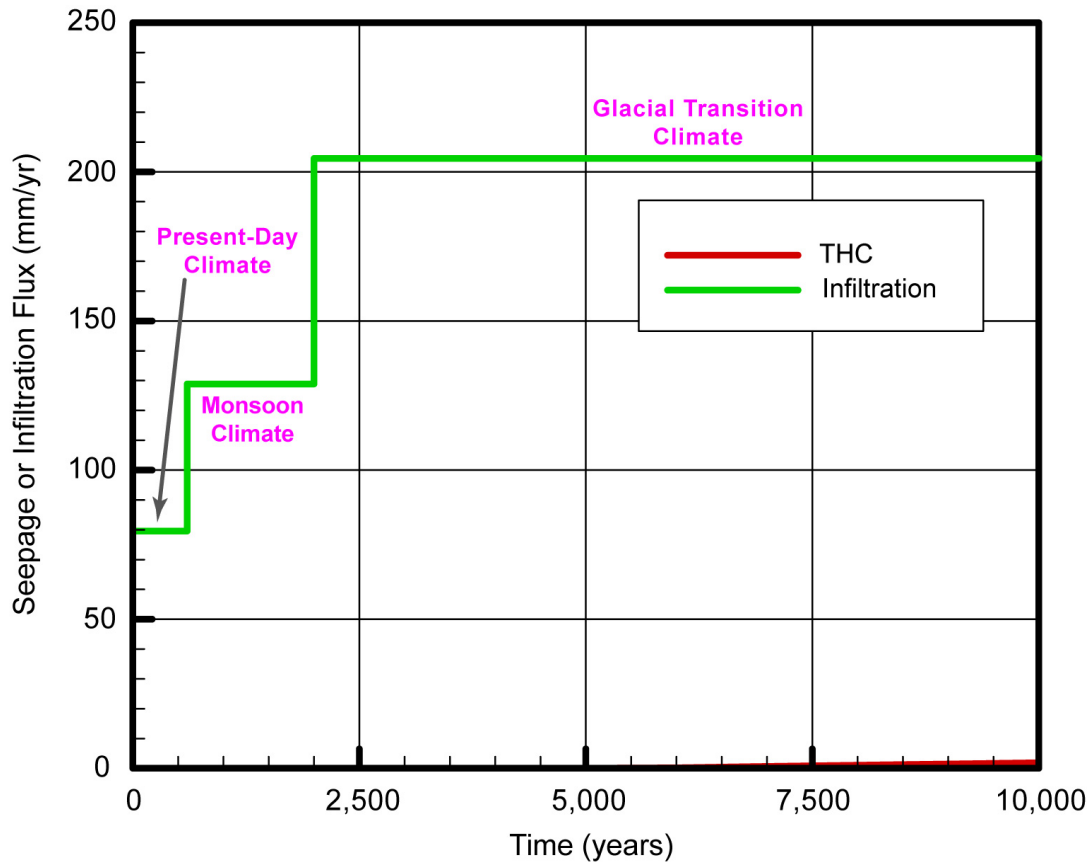
Figure 6.7-1. Comparison of Seepage Fluxes from Ambient (Simulation ID: "scm_r1_10x_nlev_amb"), TH (Simulation ID: "scm_r1_10x_nlev_th."), and THC (Simulation ID: "scm_r1_10x_nlev_thc") Simulations with Realization #1 of the Heterogeneous Fracture Permeability Distribution with IMF10 Infiltration Fluxes



Source: Output DTNs: LB0705THCSEN2.004, LB0705THCSEN2.005, and LB0705THCSEN2.006.

NOTE: See Table 6.7-1 for explanation of simulation IDs.

Figure 6.7-2. Comparison of Seepage Fluxes from Ambient (Simulation ID: "scm_r2_10x_nlev_amb"), TH (Simulation ID: "scm_r2_10x_nlev_th."), and THC (Simulation ID: "scm_r2_10x_nlev_thc") Simulations with Realization #2 of the Heterogeneous Fracture Permeability Distribution with IMF10 Infiltration Fluxes



Source: Output DTNs: LB0705THCSEN3.004, LB0705THCSEN3.005, and LB0705THCSEN3.006.

NOTES: See Table 6.7-1 for explanation of simulation IDs.

Ambient (Simulation ID: "scm_r3_10x_nlev_amb") and TH (Simulation ID: "scm_r3_10x_nlev_th.") simulations do not predict seepage. Maximum predicted seepage from THC (Simulation ID: "scm_r3_10x_nlev_thc") simulations is less than 1.9 mm/yr.

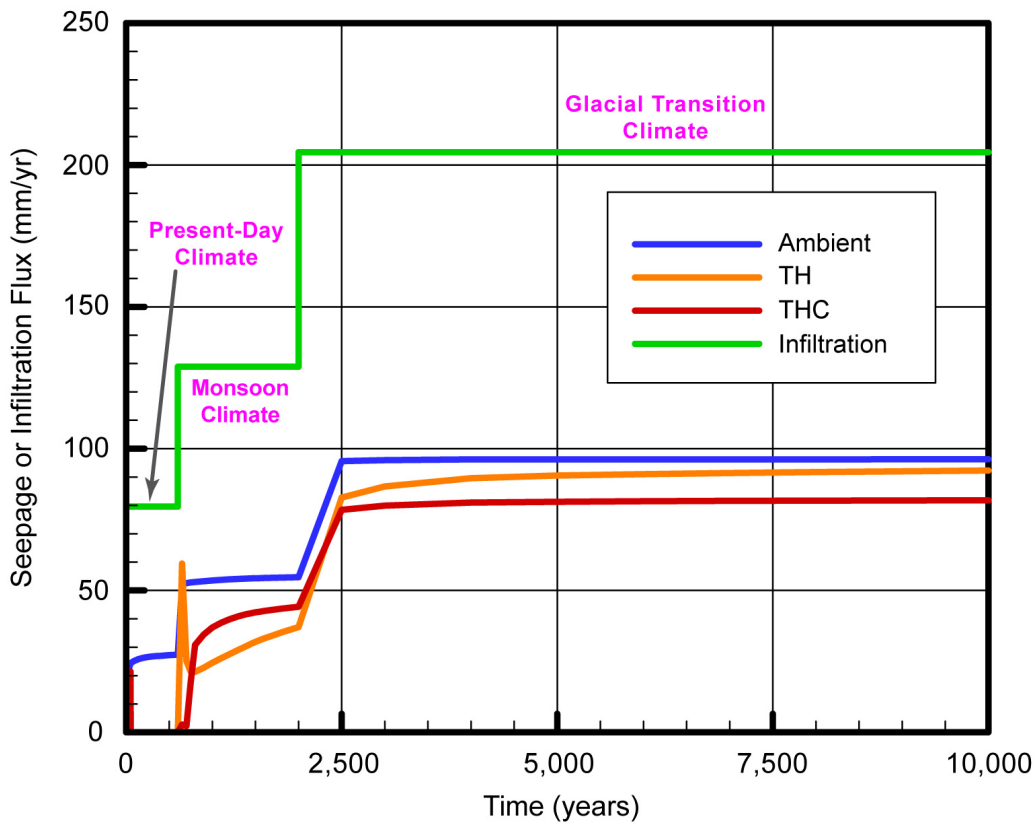
Figure 6.7-3. Seepage Fluxes from THC (Simulation ID: "scm_r3_10x_nlev_thc") Simulations with Realization #3 of the Heterogeneous Fracture Permeability Distribution with IMF10 Infiltration Fluxes

From Figures 6.7-1 through 6.7-3, a few observations can be made.

- Local fracture heterogeneity plays a key role in determining whether seepage occurs. This is clear from the different transient patterns of seepage from the three realizations of the heterogeneous fracture permeability distribution. While simulations with Realization #1 of the heterogeneous fracture permeability distribution predict considerable long-term seepage (also a spike in seepage from THC simulation), simulations with the other two realizations of the fracture permeability distribution predict almost no seepage (except for a "spike" in seepage around 600 years from THC simulations with Realization #2 of the heterogeneous fracture permeability distribution). These results are summarized in Table 6.7-3.

From Table 6.7-5, it can be seen that seepage is not predicted to occur for any of the three realizations of heterogeneous fracture permeability distribution, if IMF1 infiltration fluxes are imposed. This is true for THC simulations as well as ambient and TH simulations. In other words, for the IMF1 infiltration fluxes (7.96 mm/yr for 0 to 600 years, 12.45 mm/yr for 600 to 2,000 years, and 20.45 mm/yr for 2,000 years and beyond), the saturation buildup near the emplacement drift is not sufficient to overcome the capillary-barrier effect. This is expected because we have constrained the initial fracture capillary-strength parameter, such that seepage does not happen under ambient conditions with present-day mean infiltration fluxes (see Section 6.7.2.1 and Table 6.7-4). In addition, there is no evidence of seepage enhancement because of THC processes.

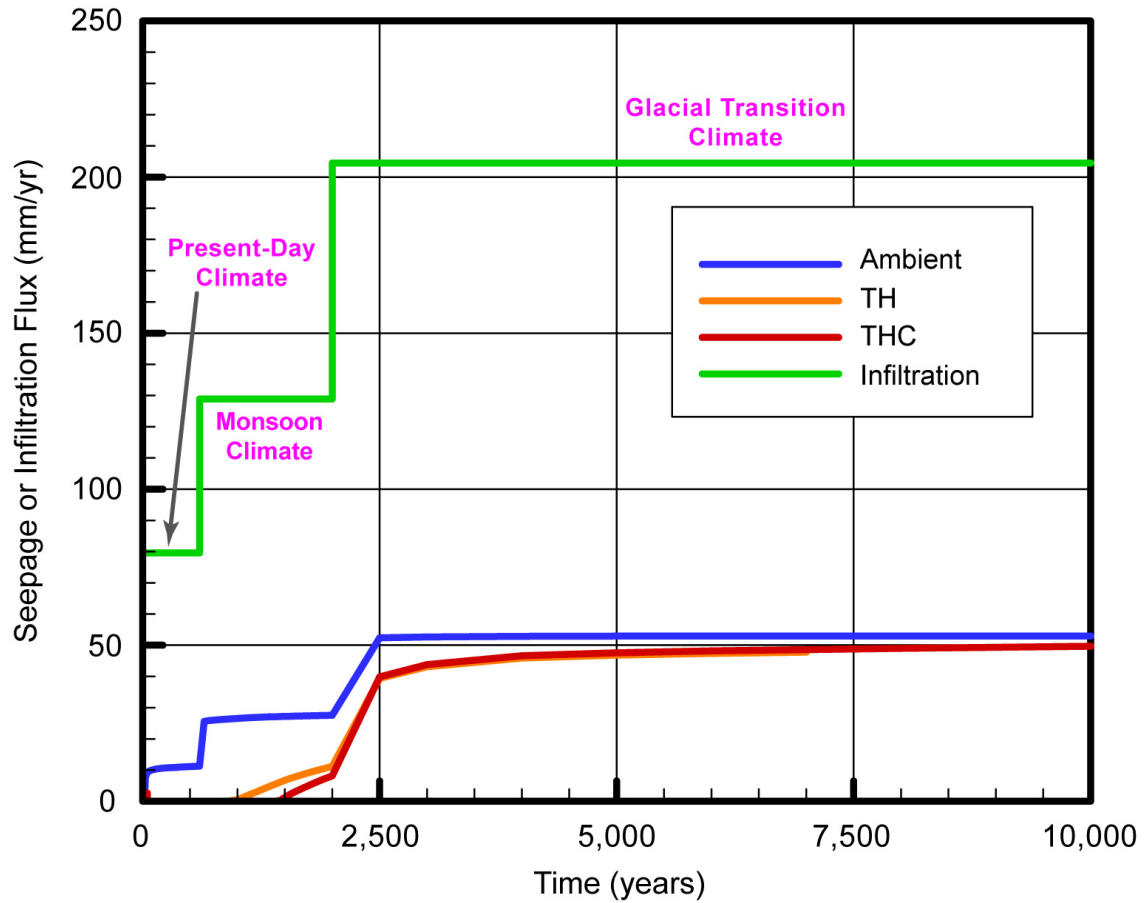
When IMF10 infiltration fluxes (79.6 mm/yr for 0 to 600 years, 128.9 mm/yr for 600 to 2,000 years, and 204.5 mm/yr for 2,000 years and beyond) are imposed on the THC seepage model (SNL 2007 [DIRS 177404]), seepage is predicted to occur. Figures 6.7-4, 6.7-5, and 6.7-6 show the seepage flux (in mm/yr) from Realizations #1, #2, and #3, respectively.



Source: Output DTNs: LB0705THCSEN1.004, LB0705THCSEN1.005, and LB0705THCSEN1.006.

NOTE: See Table 6.7-5 for explanation of simulation IDs.

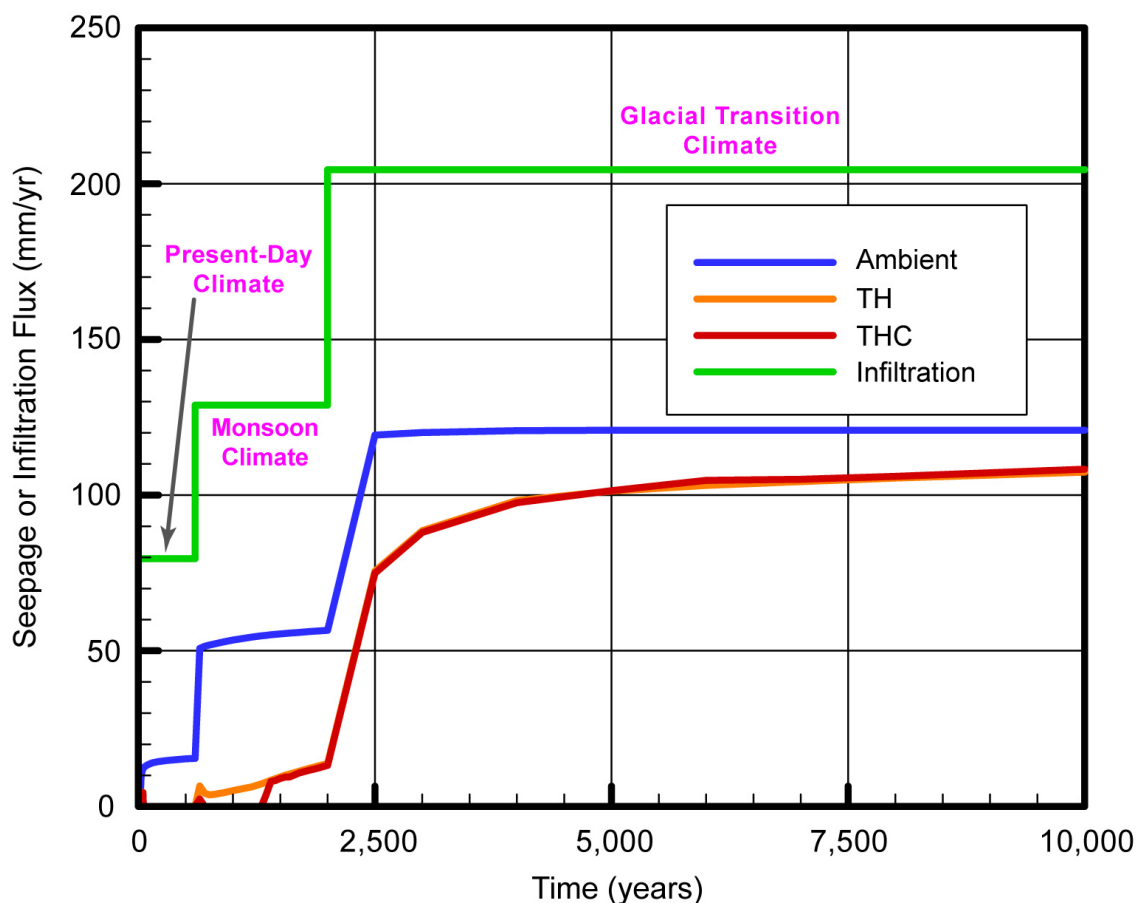
Figure 6.7-4. Comparison of Seepage Fluxes from Ambient (Simulation ID: "itr_r1_10x_lev_amb"), TH (Simulation ID: "itr_r1_10x_lev_th."), and THC (Simulation ID: "itr_r1_10x_lev_thc") Simulations with Realization #1 of the Heterogeneous Fracture Permeability Distribution and Initial Fracture Capillary-strength Parameter of 1,313 Pa (see Section 6.7.2.1 and Table 6.7-4) with IMF10 Infiltration Fluxes



Source: Output DTNs: LB0705THCSEN2.004, LB0705THCSEN2.005, and LB0705THCSEN2.006.

NOTE: See Table 6.7-5 for explanation of simulation IDs.

Figure 6.7-5. Comparison of Seepage Fluxes from Ambient (Simulation ID: "tr_r2_10x_lev_amb"), TH (Simulation ID: "itr_r2_10x_lev_th."), and THC (Simulation ID: "itr_r2_10x_lev_thc") Simulations with Realization #2 of the Heterogeneous Fracture Permeability Distribution and Initial Fracture Capillary-strength Parameter of 2,000 Pa (see Section 6.7.2.1 and Table 6.7-4) with IMF10 Infiltration Fluxes



Source: Output DTNs: LB0705THCSEN3.004, LB0705THCSEN3.005, and LB0705THCSEN3.006.

NOTE: See Table 6.7-5 for explanation of simulation IDs.

Figure 6.7-6. Comparison of Seepage Fluxes from Ambient (Simulation ID: “itr_r3_10x_lev_amb”), TH (Simulation ID: “itr_r3_10x_lev_th.”), and THC (Simulation ID: “itr_r3_10x_lev_thc”) Simulations with Realization #3 of the Heterogeneous Fracture Permeability Distribution and Initial Fracture Capillary-strength Parameter of 750 Pa (see Section 6.7.2.1 and Table 6.7-4) with IMF10 Infiltration Fluxes

As anticipated, the dynamic pattern of seepage (in terms of the magnitude of seepage flux) is different from one realization of the heterogeneous fracture permeability distribution to another (because of the local nature of the underlying physical phenomenon). However, some broad observations can be made from these simulations:

- Long-term TH and THC seepage commence well after the time when ambient seepage is applied in TSPA (BSC 2004 [DIRS 169131]) after cooldown. This happens because of the presence of the vaporization barrier effects (Birkholzer et al. 2004 [DIRS 172262]; BSC 2005 [DIRS 172232]; BSC 2006 [DIRS 174104]; Mukhopadhyay et al. 2006 [DIRS 180822]) resulting from repository heating in TH and THC seepage simulations. The actual time at which long-term seepage commences is different from one realization to another, controlled mostly by changes in infiltration fluxes resulting from climate change and the speed with which the fractures rewet (in turn controlled by the TH and

[DIRS 174104], Section 6.2.2.1.2) were conducted by holding the fracture capillary-strength parameter constant. This approach was consistent with previous seepage studies under ambient (BSC 2004 [DIRS 167652]; BSC 2004 [DIRS 171764]) or thermal simulations (Birkholzer et al. 2004 [DIRS 172262]; BSC 2005 [DIRS 172232]). The simulations in this report (see Section 6.7) demonstrate that excluding fracture capillarity heterogeneity while including permeability heterogeneity results in overprediction of local flow channeling (and seepage) in THC simulations (compared to ambient and TH simulations). To reduce this uncertainty, simulations are thus performed in this report by including heterogeneities in both fracture permeability and capillarity. To cover the range of possible initial fracture capillary-strength parameter values (since no direct experimental data are available in this instance), sensitivity studies are performed starting with initial fracture capillary-strength parameters that are themselves dependent on the specific realization of the fracture permeability distribution. Consequently, seepage results were obtained covering a large range of the initial fracture capillary-strength parameter values (750 to 2,000 Pa). These simulations improve confidence with regard to seepage estimation under THC conditions. However, a small amount of uncertainty still remains because of the unavailability of direct seepage-related data under thermal conditions.

6.11 INTENDED USE OF OUTPUTS

Results of simulations presented above are intended to provide information on the THC seepage model sensitivity to heterogeneity in fracture permeability and capillarity of the host rock (Tptpl). Heterogeneity in host rock fracture permeability was introduced by using three realizations of a heterogeneous fracture permeability distribution. The heterogeneous fracture permeability distribution created for the ambient/TH/THC simulations presented in this report was generated with the same geostatistical inputs (Table 4.1-1) as those used for generating the fracture permeability distribution in the SMPA (BSC 2004 [DIRS 167652]).

The output from this sensitivity analysis is amount of seepage, if any, into the drifts, and the time when seepage happens. It should be remembered, however, that for full consistency with previous THC seepage model simulations, simulations discussed above were run with the same input data as used in *Drift-Scale THC Seepage Model* (SNL 2007 [DIRS 177404]), except for those data on which sensitivity analyses were performed, as described in Table 4.1-1. As mentioned in Section 1.1, the objective of these sensitivity studies is to improve confidence in the abstraction of drift seepage. The sensitivity studies documented in this report provide additional information regarding the use of the THC seepage model. The products of this report may be used as direct inputs to TSPA or to any of the abstractions used by TSPA, even though they were not developed specifically for this use.

7. CONCLUSIONS

7.1 MAIN FINDINGS AND IMPLICATIONS FOR TSPA

Sensitivity studies were carried out to determine the impact of heterogeneity in fracture permeability and capillarity on the evolution of ambient/TH/THC processes in the near-field rock. These sensitivity studies were performed with the objective of determining whether the TH/THC changes in the host rock would influence the quantity and chemistry of seepage. The THC seepage model, based on the TOUGHREACT V3.1.1 reactive transport software (see Section 3.1 and Table 3-1), was used to perform these sensitivity studies. Heterogeneity in the fracture permeability of the Tptpl host rock unit in the THC seepage model was introduced by using a heterogeneous fracture permeability distribution, adopted from that used in the SMPA (BSC 2004 [DIRS 167652]) for the sake of consistency with the ambient seepage models. Heterogeneity in fracture capillarity of the host rock was considered through two processes: (1) considering the impact of fracture permeability heterogeneity on fracture capillarity through Leverett scaling relations (Section 6.3); and (2) using different initial fracture capillary-strength parameters for different realizations of the same fracture permeability distribution, covering a wide range of fracture capillary-strength parameters.

The fracture capillary-strength parameter of the host rock is a critical factor in determining whether seepage will occur. In the base-case simulations presented in this report, the fracture capillary-strength parameter was adopted from *Calibrated Unsaturated Zone Properties* (SNL 2007 [DIRS 179545]) (see Section 6.4.11.4 of the present report, which justifies this selection). Additional simulations were performed where the fracture capillary-strength parameter was either from the SCM (to demonstrate the impact on seepage of not including capillary heterogeneity while including permeability heterogeneity) or from iterative ambient simulations, which determined the minimum fracture capillary-strength parameter that would prevent ambient seepage. These iterative simulations were further supported by analyses of synthetic liquid-release test data (see Sections 6.4.11.3 and 6.4.11.4), which also demonstrated the impact of dimensionality (3-D vs. 2-D), scale (small-scale fractures near the emplacement drifts vs. fracture continuum encompassing the entire host rock unit), and the calibration method employed (including or excluding Leverett-scaling effects in the calibration model) on the estimated fracture capillary-strength parameter. The analyses in Section 6.4.11.3 indicated that the calibrated (inclusive of Leverett scaling) effects have a large standard deviation, pointing to the local nature of the phenomenon (local permeability heterogeneity has a strong impact on the estimated fracture capillary-strength parameter). As a result, sensitivity studies (which included Leverett-scaling effects) were performed in this report covering a large range of initial fracture capillary-strength parameters.

Seepage into the drifts, of course, is also determined by the infiltration fluxes. In the sensitivity studies of this report, two sets of infiltration fluxes were used to demonstrate whether or not seepage occurs, and if it does occur, to predict its quantity and chemistry. The complete suite of simulations performed is listed in Tables 6.5-1 (steady-state simulations), 6.5-2 (base-case simulations), 6.7-1 (simulations with SCM fracture capillary-strength parameter and without Leverett-scaling effects), 6.7-4 (iterative ambient simulations), and 6.7-5 (simulations with heterogeneity in both fracture permeability and capillarity). For each of these parameter combinations (different realizations of the heterogeneous fracture permeability distribution,

[DIRS 174104]; Mukhopadhyay et al. 2006 [DIRS 180822]), where heterogeneity in fracture capillarity was not accounted for.

The more important observation was that ambient seepage was larger than either TH or THC seepage. These findings partially address the concerns expressed in CR-7037. The results in this report suggest that the anomalous THC seepage predicted by *THC Sensitivity Study of Repository Edge and Heterogeneous Permeability Effects* (BSC 2006 [DIRS 174104]) was the result of not including an important physical process (Leverett scaling). The findings in this report also suggest that seepage abstraction methodology can be based on ambient seepage rates, and no change in the seepage abstraction procedure is necessary because of THC-related processes.

Based on the sensitivity simulations performed in this report, it is concluded that Leverett-scaling effects influence the overall seepage rate. The seepage abstraction procedure (BSC 2004 [DIRS 169131]) does not include Leverett-scaling effects. However, the abstraction procedure (BSC 2004 [DIRS 169131]) uses the fracture capillary-strength parameter from the SCM (BSC 2004 [DIRS 171764]), which also does not include Leverett-scaling effects, thereby providing a consistent basis for abstraction. As the discussion in Section 6.4.11.3 indicates, if the liquid-release test data from the SCM (BSC 2004 [DIRS 171764]) were to be calibrated including Leverett scaling, a different (likely larger) fracture capillary-strength parameter value would be obtained. This newly calibrated fracture capillary-strength parameter value should be used in seepage prediction, if the abstraction were to include Leverett-scaling effects. On the other hand, using the SCM (BSC 2004 [DIRS 171764]) calibrated fracture capillary-strength parameter in an abstraction procedure that includes Leverett scaling would lead to inconsistent results.

In summary, the main conclusions from this report are (1) if only heterogeneity in fracture permeability is considered without consideration of corresponding heterogeneity in fracture capillarity, seepage from THC simulations may be predicted that is larger than ambient seepage (because of an overprediction of local flow channeling effects), (2) when both fracture capillarity and permeability heterogeneity is included in the conceptual model, ambient seepage is expected to be larger than TH or THC, (3) abstraction of drift seepage may be based on ambient seepage and no change in abstraction procedure is necessary because of THC-induced processes, and (4) Leverett scaling plays an important role in controlling seepage. If seepage abstraction were to include Leverett-scaling effects, seepage testing data would have to be recalibrated.

7.2 UNCERTAINTIES AND RESTRICTIONS FOR SUBSEQUENT USE

Uncertainties related to sensitivity analyses presented in this report are discussed in Section 6.10. The intended use of outputs from this report has been discussed in Section 6.11. Uncertainties regarding model results and restrictions for use are the same as for the THC seepage model simulations (SNL 2007 [DIRS 177404]). The objective of this work is to increase confidence in the abstraction of drift seepage (BSC 2004 [DIRS 169131]), which supports TSPA (Section 1.1). The sensitivity studies documented in this report also provide additional information regarding the use of the drift-scale THC seepage model. While the products of this report were not developed specifically for use as direct inputs to TSPA or to any of the abstractions used by TSPA, they may be used as such.

For full consistency with original THC seepage model simulations (SNL 2007 [DIRS 177404]), sensitivity analyses presented in this report were run with the same input data as used in *Drift-Scale THC Seepage Model* (SNL 2007 [DIRS 177404]), except for those parameters on which sensitivity analyses were performed. Additional sensitivity studies could further improve confidence in seepage calculations. For example, additional calculations (including recalibration to seepage testing data) could be used to estimate the initial fracture capillary strength parameter to be used in simulations that include Leverett-scaling effects from THC processes. Computing resources permitting, a limited number of 3-D THC sensitivity studies could also provide additional confidence. Notwithstanding these opportunities to further increase model confidence, the primary conclusions of this report would not be expected to change significantly.

7.3 ASSOCIATED CRS

As stated in Section 4.2, the TWP (SNL 2007 [DIRS 179287], Sections 1.2.1 and 1.2.4) specifies that this analysis report address two CRs, CR-7037 and CR-7193. In the following, a summary is provided on how these CRs have been addressed in this report.

7.3.1 CR-7037

CR 7037 notes that information provided in Revision 00 of the THC sensitivity study (BSC 2006 [DIRS 174104]) shows that predicted seepage is enhanced by THC effects not considered in *Abstraction of Drift Seepage* (BSC 2004 [DIRS 169131]). Results available from this report show that the enhancement of seepage due to THC processes, as reported in *THC Sensitivity Study of Repository Edge and Heterogeneous Permeability Effects* (BSC 2006 [DIRS 174104]) and in the study by Mukhopadhyay et al. (2006 [DIRS 180822]), happened because certain physical processes were not included in the predictive models. More specifically, the overprediction of THC seepage in the earlier reports (BSC 2006 [DIRS 174104]; Mukhopadhyay et al. 2006 [DIRS 180822]) was a result of excluding fracture capillarity heterogeneity, while including heterogeneities in fracture permeability and dynamic changes in porosities in the predictive models. The following results from this report confirm the above finding.

1. Qualified and software TOUGHREACT V3.1.1 (see Section 3.1 and Table 3-1) has been used in performing the simulations in this report.
2. Though the values of infiltration fluxes and rock thermal, hydrological, and chemical properties used in this report are different from those used in *THC Sensitivity Study of Repository Edge and Heterogeneous Permeability Effects* (BSC 2006 [DIRS 174104]), the physical and chemical processes modeled in the simulations in Section 6.7.1 are the same as those in the earlier report (BSC 2006 [DIRS 174104]). The results (see Figures 6.7-1 through 6.7-3) in Section 6.7.1, derived from simulations, which exclude Leverett-scaling effects and use the SCM calibrated fracture capillary strength parameter value, are similar to those in the earlier report (BSC 2006 [DIRS 174104], Section 6.2.3.4 and Figure 6.2-11). Figures 6.7-1 through 6.7-3 thus confirm the findings of *THC Sensitivity Study of Repository Edge and Heterogeneous Permeability Effects* (BSC 2006 [DIRS 174104], Section 6.2.3.4 and Figure 6.2-11). In other words, when heterogeneity in fracture permeability is included in any predictive model while ignoring the